Differential Contributions of Microglial and Neuronal IKKβ to Synaptic Plasticity and Associative Learning in Alert Behaving Mice

Vasiliki Kyrargyri,[1] Germán Vega-Flores,[2] Agnès Gruart,[2] José M. Delgado-García,[2] and Lesley Probert[1]

Microglia are CNS resident immune cells and a rich source of neuroactive mediators, but their contribution to physiological brain processes such as synaptic plasticity, learning, and memory is not fully understood. In this study, we used mice with partial depletion of IκB kinase β, the main activating kinase in the inducible NF-κB pathway, selectively in myeloid lineage cells (mIKKβKO) or excitatory neurons (nIKKβKO) to measure synaptic strength at hippocampal Schaffer collaterals during long-term potentiation (LTP) and instrumental conditioning in alert behaving individuals. Resting microglial cells in mIKKβKO mice showed less Iba1-immunoreactivity, and brain IL-1β mRNA levels were selectively reduced compared with controls. Measurement of field excitatory postsynaptic potentials (fEPSPs) evoked by stimulation of the CA3-CA1 synapse in mIKKβKO mice showed higher facilitation in response to paired pulses and enhanced LTP following high frequency stimulation. In contrast, nIKKβKO mice showed normal basic synaptic transmission and LTP induction but impairments in late LTP. To understand the consequences of such impairments in synaptic plasticity for learning and memory, we measured CA1 fEPSPs in behaving mice during instrumental conditioning. IKKβ was not necessary in either microglia or neurons for mice to learn lever-pressing (appetitive behavior) to obtain food (consummatory behavior) but was required in both for modification of their hippocampus-dependent appetitive, not consummatory behavior. Our results show that microglia, through IKKβ and therefore NF-κB activity, regulate hippocampal synaptic plasticity and that both microglia and neurons, through IKKβ, are necessary for animals to modify hippocampus-driven behavior during associative learning.

GLIA 2014;00:000–000

Key words: microglia, NF-κB activity, conditional knockout mice, synaptic plasticity, behavior

Introduction

Microglia are resident CNS macrophages that mediate immune responses following infection and injury (Ransohoff and Brown, 2012; Kettenmann et al., 2011; Neumann et al., 2009). Microglia are also important for synaptic pruning and the maturation of neuronal circuitry during development (Schafer et al., 2012; Paolicelli et al., 2011) and increasing evidence indicates that they perform important roles in the adult brain under nonpathological conditions. Intravital time-lapse two-photon imaging in cell-specific fluorescence reporter mice showed that microglial processes are highly motile (Nimmerjahn et al., 2005; Davalos et al., 2005), making frequent contacts with neuronal synapses in the visual cortex in an activity-dependent way (Wake et al., 2009; Tremblay et al., 2010). Microglia act to reduce neuronal activity in zebrafish optic tectum (Li et al., 2012) and mouse hippocampal neurons (Ji et al., 2013). Several lines of evidence indicate that microglia play a functional role in synaptic plasticity and cognition, mainly from studies of microglial cytokines IL-1β (Schneider et al., 1998) and TNF (Stellwagen and Malenka, 2006), and of brain slices from mice deficient in microglial receptors or their ligands which show impairment of LTP and cognitive function (Rogers et al., 2011; Costello et al., 2011; Roumier et al., 2004).

View this article online at wileyonlinelibrary.com. DOI: 10.1002/glia.22756

Published online Month 00, 2014 in Wiley Online Library (wileyonlinelibrary.com). Received May 5, 2014, Accepted for publication Sep 12, 2014.

Address correspondence to Lesley Probert, Laboratory of Molecular Genetics, Hellenic Pasteur Institute, 127 Vassilissis Sophias Ave., Athens 11521, Greece. E-mail: lesley@pasteur.gr or Jose M. Delgado-Garcia, Division of Neurosciences, Pablo de Olavide University, Seville 41013, Spain. Email: jmdelgar@upo.es

From the [1]Laboratory of Molecular Genetics, Hellenic Pasteur Institute, Athens 11521, Greece; [2]Division of Neurosciences, Pablo de Olavide University, Seville 41013, Spain.

Additional Supporting Information may be found in the online version of this article.

However, since gene expression in cell types other than microglia may be altered in conventional gene knockout mice and the preparation of brain slices can inherently activate microglia, direct evidence for a role of microglia in synaptic plasticity and cognitive function has remained elusive.

NF-κB is a ubiquitous, dynamically regulated transcription factor expressed by CNS neurons and all glial cell types. It induces the expression of growth factors, cytokines, and anti-apoptotic molecules and thereby promotes immune functions of glia and cell survival in neurons (Kaltschmidt and Kaltschmidt, 2009). NF-κB is constitutively active in neurons and was originally thought to play a cell-autonomous role in the modulation of synaptic function (Mattson and Camandola, 2001; Meffert et al., 2003). Spatial memory and late LTP were reduced in mice with an inducible deficiency of NF-κB activity in glutamatergic neurons (Fridmacher et al., 2003; Kaltschmidt et al., 2006), and correspondingly increased in mice with a similar deficiency mainly in GABAergic neurons (O'Mahony et al., 2006). NF-κB is inducibly expressed by CNS glia, and astrocyte-specific NF-κB activity was shown to contribute to spatial learning and fear memory (Bracchi-Ricard et al., 2008). However, the role of microglial NF-κB in the brain under nonpathological conditions has not been investigated.

In this study, we directly compared microglial and neuronal NF-κB function in the hippocampus of alert behaving mice by recording synaptic strength at hippocampal CA3-CA1 synapses during LTP and instrumental conditioning in mice with cell-specific depletion of the inhibitor of κB kinase β (IKKβ), the main NF-κB-activating kinase in the inducible pathway (Vallabhapurapu and Karin, 2009), in cells of myeloid lineage or excitatory neurons. We show that microglial and neuronal IKKβ are differentially required in the regulation of hippocampal neuronal activity but both independently contribute to associative learning of hippocampus-dependent appetitive behavior.

Materials and Methods

Mice

Mice containing a conditional IKKβ allele in which exon 3 of the *Ikbkb* gene, encoding the IKKβ activation loop, is flanked by loxP sites ($IKK\beta^{F/F}$) have been described previously (Park et al., 2002; Li et al., 2003). Mice with a selective depletion of IKKβ in CNS neurons (nIKKβKO) were generated by crossing $IKK\beta^{F/F}$ mice with transgenic mice that express a neuronal CamKII promoter-driven Cre recombinase (CamKII-Cre) (Minichiello et al., 1999) and have been characterized previously (Emmanouil et al., 2009). Mice with a selective depletion of IKKβ in cells of myeloid origin (mIKKβKO) were generated by crossing $IKK\beta^{F/F}$ mice with transgenic mice that express a CD11b promoter-driven Cre recombinase (CD11b-Cre; Fig. 1). Controls referred to throughout this manuscript are $IKK\beta^{F/F}$ mice. All mice were backcrossed onto the C57BL/6 genetic background for at least seven generations. Mice were generated and bred under specific pathogen-free conditions in the experimental unit of the Hellenic Pasteur Institute and male mice were transferred to the Pablo de Olavide University Animal House 2 weeks before the beginning of the experiments. Animals were kept on a 12 h light/dark cycle with constant ambient temperature ($21 \pm 1.5°C$) and humidity ($55 \pm 10\%$). Food and water were available *ad libitum*. Experiments were performed in adult (3–5 months old; 25–30 g) male mice under specific housing conditions (no females in the same building, sound- and vibration-proof). All electrophysiological and behavioral studies were performed in accordance with European Union (2010/63/EU) guidelines and Spanish (BOE 34/11370-421, 2013) regulations for the use of laboratory animals in chronic experiments. The experimental protocols were also approved by the local ethics committee of the Pablo de Olavide University (Seville, Spain).

Isolation of Primary Microglial Cells, Astrocytes, and Peritoneal Macrophages

Primary mixed astrocytes/microglia cultures were prepared following procedures described elsewhere (Lee et al., 2000). Briefly, the cultures were prepared from individual postnatal day 1–3 mIKKβKO and control mice, which were concurrently genotyped by tail biopsy. After removing meninges from the cerebral hemispheres, tissue (cortex and hippocampus) was dissociated into a single-cell suspension by gentle trituration. Cells were cultured in glial culture media (high glucose DMEM supplemented with 10% FBS, 10% HS, 2 mM L-glutamine and 1 mM PenStrep) in 25 cm^2 flasks (poly-L-lysine coated) at 37°C in a 5% CO_2 incubator. The medium was supplemented with GM-CSF (5 ng/mL, Cat # G0282, Sigma-Aldrich) for enhancing microglial growth and was changed every 3 days. At DIV (days *in vitro*) 14, floating microglia were collected from the mixed cultures by shaking the flasks at 200 rpm at 37°C for 4–5 h. The supernatants with the floating microglia were collected, centrifuged at 900 rpm for 5 min and seeded in 12-well plates (5×10^5 cells/well), and used for protein isolation 2–3 days later. Microglial cell lysates were collected from untreated cells or cells treated with LPS (10 μg/mL) for 30 min at 37°C. The remaining astrocytes were supplemented with fresh glial culture medium and were used as controls. The presence of microglial cells in the remaining astrocyte cultures was estimated to be 27% while microglia enrichment in microglial cell cultures was estimated to be ≥95%, as determined by FACS analysis using an antibody to the myeloid cell lineage marker CD11b (see Supp. Info. Material and Methods and Fig. 1). Peritoneal macrophages were harvested by peritoneal lavage from adult mIKKβKO and control mice that had received 1 mL of 4% thioglycollate medium (Difco, Cat # 225650, Becton Dickinson) i.p. 3 days previously. Cells were washed once in RPMI containing 10% FBS and allowed to adhere to 6-well plates by incubation for 45 min at 37°C in a 5% CO_2 incubator.

Western Blot Analysis

Twenty-five micrograms of total protein extracts from microglia, astrocytes, peritoneal macrophages, and brain tissues (whole brain, cerebellum, cortex, and hippocampus) were resolved on NuPAGE Novex Bis-Tris Gels (Invitrogen, Cat # NP0321) and transferred onto nitrocellulose membranes (Schleicher and Schuell). Blots were probed with antibodies to IKKβ (1:1000, L570, Cell Signaling

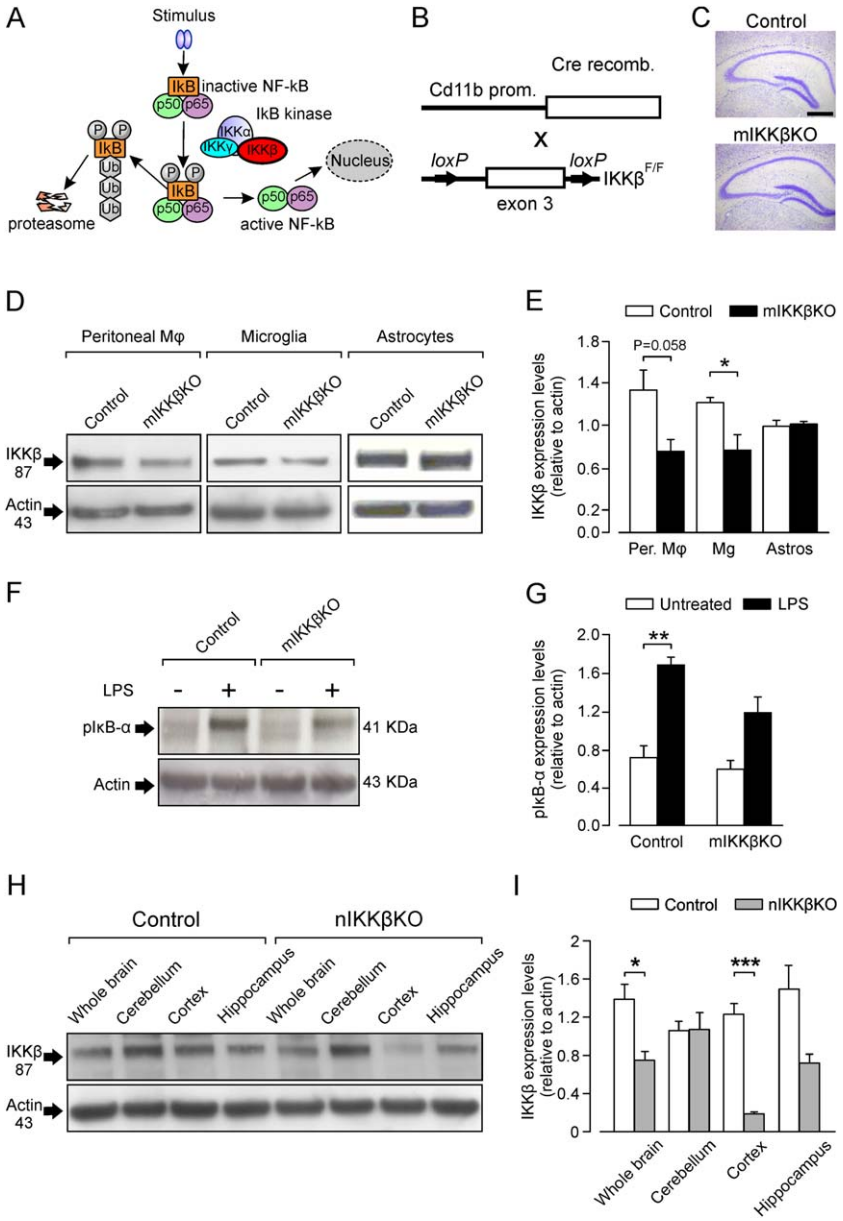

FIGURE 1: mIKKβKO mice show selective depletion of IKKβ and NF-κB signaling in cells of myeloid origin. (A) Schematic representation of IKKβ-mediated NF-κB activation. (B) Schematic representation of the targeting strategy followed for the generation of mIKKβKO mice which carry a CD11bCre transgene and two mutant IKKβ alleles in which exon 3 is flanked by loxP sites ($IKK\beta^{F/F}$). Control mice carry loxP-flanked IKKβ alleles only ($IKK\beta^{F/F}$). (C) Photomicrographs illustrating the hippocampal formation (Nissl staining) in control and mIKKβKO mice. Scale bar, 250 μm. (D) Representative Western blot showing IKKβ production by peritoneal macrophages ($n = 5$ mice per group), microglia ($n = 4$ mice per group), and astrocytes ($n = 4$ mice per group) isolated from mIKKβKO and control mice. Actin is shown as a loading control. (E) Quantitative analysis of the immunoblots shown in D (*$P = 0.045$, Mann-Whitney test). Abbreviations: Per. Mφ, peritoneal macrophages; Mg, microglia; Astros, astrocytes. (F) Representative Western blot showing phospho IκB-α production by microglial cells isolated from mIKKβKO and control mice, with (+) and without (−) stimulation with LPS (10 μg/mL) for 30 min. Actin is shown as a loading control. (G) Quantitative analysis of the immunoblots shown in F ($n = 3$ microglial cultures per group, **$P = 0.005$, t test). (H) Representative Western blot showing IKKβ production in protein lysates from different brain regions, of nIKKβKO and control mice. Actin is shown as a loading control. (I) Quantitative analysis of the immunoblots shown in H ($n = 3$ mice per group) (*$P = 0.045$, ***$P = 0.001$, t test). [Color figure can be viewed in the online issue, which is available at wileyonlinelibrary.com.]

Technology, Cat # 2678, RRID: AB_2122301), phospho-IκB-α (1:500, Cell Signaling Technology, Cat # 9241), IL-1β (1:200, Santa Cruz biotechnology, Cat # sc-7884), and EAAT2 (see Supp. Info. Fig. 4) (1:200, Santa Cruz biotechnology, Cat # sc-15317) followed by horseradish peroxidase-conjugated anti-rabbit IgG (1:2000, Cat # 111-035-003, Jackson Immunoresearch Laboratories, RRID: AB_2313567). Antibody binding was detected using the ECL Prime detection system (Amersham Pharmacia, Cat # RPN2232). To

normalize for protein content, membranes were stripped and reprobed with anti-actin antibody (1:5000, Millipore, Cat # MAB1501, RRID: AB_2223041). Quantification of the protein expression levels was done using the Image-J software.

RNA Isolation and Quantitative RT-PCR

Total RNA was extracted from brain and spinal cord tissues using TRIzol (Invitrogen, Paisley, UK) according to the manufacturer's instructions. DNAse-treated RNA samples were analyzed by quantitative RT-PCR using QuantiFast™ SYBR® green RT-PCR kit (Qiagen Inc.) according to the manufacturer's instructions. All reactions were performed using a LightCycler (Roche, Mannheim, Germany). At the end of each PCR run, melting curve analysis was also performed to verify the integrity and homogeneity of PCR products. Gene expression levels were calculated using standard curves for each gene, which were created by plotting threshold cycle (CT) values versus the logarithm of serial-diluted RNA concentrations. A least squares method was used for the determination of A and B values in the equation $CT = A^*Log(C_{RNA}) + B$. The coefficient of determination (R^2) was greater than 0.99. Values were normalized using the respective values for the chosen housekeeping genes, *Gapdh* and *Actb*. Only values normalized against *Gapdh* are shown in this manuscript, however normalizations against *Actb* showed similar results (Supp. Info. Fig. 2). All results were analyzed using the LightCycler software version 3.5 (Roche, Mannheim, Germany, RRID: rid_000088). QuantiTect Primer Assays were used for *Il6* (Mm_Il6_1_SG), *Il1b* (Mm_Il1b_2_SG), *Tnf* (Mm_Tnf_1_SG), *Nos1* (Mm_Nos1_2_SG), *Nos2* (Mm_LOC673161_1_SG), *Actb* (Mm_Actb_2_SG), and *Gapdh* (Mm_Gapdh_3_SG) (Qiagen).

Electrode Implantation

Animals were anaesthetized with 0.8%–1.5% isoflurane and implanted with bipolar stimulating electrodes in the right Schaffer collateral/commissural pathway of the hippocampus, a recording electrode in the ipsilateral CA1 pyramidal layer and a ground wire affixed to the bone of the skull, as previously described (Gruart et al., 2012; Jurado-Parras et al., 2013) (Fig. 3A, B). The final location of the recording electrode was confirmed by the presence of reliable monosynaptic fEPSPs evoked by paired pulses (40 ms interpulse interval) presented to Schaffer collaterals. After surgery, animals were returned to their home cages to recover at least 7 days before the beginning of the electrophysiology recordings.

In Vivo Electrophysiology Recordings

Animals were prepared according to procedures described elsewhere (Gruart et al., 2012). Animals were placed in separate, small (5 × 5 × 10 cm) plastic chambers located inside a larger Faraday box (30 × 30 × 20 cm). fEPSPs were recorded with the help of Grass P511 differential amplifiers (Grass Instruments, Warwich, RI, USA) through high-impedance probes (2×10^{12} Ω, 10 pF). Recording sessions were performed with six animals at a time. All the *in vivo* recordings were made in awake, non-anaesthetized animals.

Input/Output (I/O) Curves. To investigate basal synaptic transmission properties we measured input/output responses by stimulating the Schaffer collaterals with paired pulses (40 ms of interstimulus intervals) at increasing intensities (0.02–0.4 mA, in steps of 0.02 mA, ≈10 paired pulses each intensity) (Figs. 3C and 4A).

Paired Pulse Facilitation. To evaluate synaptic function we induced paired pulse facilitation (PPF), a form of short-term plasticity that measures the probability of neurotransmitter release from the presynaptic terminal. We checked the effects of paired pulses at different (10, 20, 40, 100, 200 and 500 ms) interstimulus intervals using intensities corresponding to 30% - 40% of the amount required to evoke a saturating response (Figs. 3D and 4B). In all cases, the pair of pulses of a given intensity was repeated at least five times with time intervals ≥30 s, to avoid as much as possible interference with slower short-term potentiation (augmentation) or depression processes (Zucker and Regehr, 2002).

Long Term Potentiation. To further investigate synaptic function we induced LTP, a form of long-term plasticity that is thought to underlie the processes of learning and memory. To evoke LTP in behaving mice, we followed procedures described elsewhere (Gruart et al., 2012). fEPSP baseline values were collected 15 min before LTP induction using paired (40 ms interstimulus intervals) 100 μs, square, and biphasic pulses (Figs. 3E and 4C). Pulse intensity was set at 35% of the amount necessary to evoke maximum fEPSP response (0.15–0.25 mA), which is below the threshold for evoking a large population spike. An additional criterion for selecting stimulus intensity was that the second stimulus should evoke a larger (>20%) fEPSP than the first. For LTP induction, animals were presented with an HFS session consisting of five 200 Hz, 100 ms trains of pulses at a rate of 1 min. Thus, a total of 600 pulses were presented during an HFS session. To avoid evoking population spikes and/or the appearance of local seizures, the stimulus intensity during HFS was set at the same as that used for generating baseline recordings. Animals that presented discharges or motor seizures after the HFS protocol (as checked by online electroencephalographic (EEG) recordings and visual observation of the stimulated animal) were excluded from the study. The HFS session was repeated for the first 2 consecutive days. After the HFS sessions, the same paired-pulse stimuli (40 ms interstimulus interval) were presented every 20 s for 60 min and for 30 min the 4 following days. For the analysis of the data, we measured both the amplitude and the slope of the first fEPSP recorded throughout the different sessions. Only fEPSP amplitudes are shown in this manuscript, however analysis of the slopes showed similar results.

Behavioral Analysis

Rotarod. Age-matched mice ($n = 14$ per group) were tested for overall balance, motor coordination and motor learning using a rotarod apparatus (UgoBasile, Comerio, Italy) following procedures described elsewhere (Madroñal et al., 2010). Mice were placed on the rod and tested at an accelerating speed of 2–20 rpm over a maximum of 300 s on each of 4 consecutive days. Each mouse performed two trials per day with a time interval of 1 h between them. During that period and between the experimental days mice were allowed to recover in their home cages. Mice were tested for the time spent on the rod, which was recorded automatically by a trip switch located at the floor of each rotating drum, and considered as the latency

time to fall. The results obtained from the two trials on each day were averaged to obtain a single value for each group and session and this value is referred as mean latency time to fall.

Open Field Task. The open field test was used to test general exploratory activity (total distance traveled) and levels of anxiety (time spent in center vs. periphery). Animals ($n = 14$ per group) were monitored in an automated 40 cm square open arena with 30 cm walls (ACTIFOT 809, Cibertec, Madrid, Spain) for 15 min according to procedures described elsewhere (Valles-Ortega et al., 2011). Horizontal locomotor activity and center time exploration were measured later by a monitor-recognition software (Smart Junior, Panlab, Barcelona, Spain, RRID: rid_000087). A square central area accounting for 16% of the total area was defined as "center."

Passive Avoidance Task. The passive avoidance test was used to test contextual fear learning and memory. It was carried out in a passive avoidance device for mice (UgoBasile, Comerio, Italy) in accordance to procedures described elsewhere (Potter et al., 2010). Each mouse ($n = 13$ controls, $n = 13$ mIKKβKO, and $n = 14$ nIKKβKO mice) was placed in the illuminated part of the device, which was connected to the dark part of the same size that was fitted with an electric grid floor. The two parts were separated by an automatic door that was opened 10 s after the placement of each mouse to the illuminated part. During the acquisition session, entrance of the mouse into the dark part was punished by an electric foot shock (0.6 mA, 3 s). After 1, 24, and 48 h, pretrained mice were placed again in the illuminated part of the device and observed for up to 300 s. The time spent in the illuminated part after the training period is considered as the latency time and mice that avoided the dark part during the whole time of experiment were considered to remember the task to the maximum level (300 s).

Instrumental Conditioning Task

Associative learning was tested using the instrumental conditioning paradigm, and consisted of two different protocols labeled as Instrumental test I and Instrumental test II. Training took place in Skinner box modules measuring 12.5 × 13.5 × 18.5 cm (MED Associates, St. Albans, VT, USA), as we have described elsewhere (Jurado-Parras et al., 2013; Madroñal et al., 2010) (Fig. 6). Each Skinner box was housed within a sound-attenuating chamber (90 × 50 × 60 cm) exposed to a 45 dB white noise (Cibertec, Madrid, Spain). The Skinner box was equipped with a food dispenser from which pellets (MLabRodent Tablet, 20mg; Test Diet, St. Louis, MO, USA) were delivered by pressing a lever. Before training, mice were handled daily for 7 days and food deprived to 75%-85% of their free-feeding weight.

Instrumental Test I. Animals were first trained, in 20 min sessions, to press the lever to receive pellets from the feeder using a fixed-ratio (1:1) schedule (Fig. 6B, top). Animals were trained until they reached a selected criterion of obtaining ≥20 pellets per session for two successive sessions, as previously described (Hasan et al., 2013). Once reaching the criterion, mice were trained in a more complex task (light/dark paradigm). Here, only lever presses performed during a light period (20 s) were reinforced with a pellet; lever presses during the dark period (20 ± 10 s) were not reinforced and restarted the dark period for an additional random time (1–10 s) (Fig. 6B, bottom). For the light/dark paradigm, the Skinner box was fitted with a small house light (3 W) mounted above the lever.

Instrumental Test II. Mice with permanently implanted electrodes in the Schaffer collateral pathway of the right hippocampus were trained using the fixed-ratio (1:1) schedule only. In this case, the Skinner box was fitted with a Perspex wall separating the lever from the feeder. fEPSP recordings were carried as indicated above. Electrical stimuli presented to Schaffer collaterals consisted of a single 100 μs, square, and biphasic pulse. Stimulus intensities ranged from 0.02 to 0.2 mA. During the Instrumental test II, animals were presented with simple pulses at Schaffer collaterals immediately before the daily sessions (pre-session recordings), inside a plastic box located temporarily inside the Skinner box (Fig. 7B), and when performing the following behaviors during instrumental conditioning sessions: "going-to-lever" (appetitive behavior) and "going-to-feeder" (consummatory behavior), according to the procedures described elsewhere (Jurado-Parras et al., 2013). "Going-to-lever" and "going-to-feeder" were determined with the help of photoelectric cells located 5 cm from the lever and the feeder (Fig. 7A, D). Electrical stimulations left a marker in both the electrical recording and video-capture systems. This marker was distinct between the appetitive and consummatory behaviors and fEPSPs evoked by stimuli not well synchronized with one of the two experimental behaviors were rejected before the quantitative analysis.

Conditioning programs, lever presses, and delivered reinforcements were monitored and recorded by a computer, using a MED-PC program (MED Associates, RRID: rid_000089). All of the instrumental conditioning sessions were recorded with a video-capture system (Sony HDR-SR12E, Madrid, Spain) synchronized to fEPSP recordings. Similar to I/O, PPF, and LTP analysis procedure described above, for the analysis of the instrumental box electrophysiology data, we measured both the amplitude and the slope of the fEPSPs recorded throughout the different sessions. Only fEPSP amplitudes are shown in this manuscript, however analysis of the slopes showed similar results.

Histology

Mice were transcardially perfused, under deep anesthesia (4% chloral hydrate solution, 10 mL/kg), with ice-cold saline followed by 4% phosphate-buffered paraformaldehyde (PFA). Brains were removed and post-fixed in the same fixative overnight at 4°C. To determine the location of the stimulating and recording electrodes, frozen coronal sections (20 μm) including the dorsal hippocampus were collected on gelatinized glass slides and stained by the Nissl technique (Fig. 3B).

Localization of microglia was performed in paraffin brain sections (5 μm) taken from mIKKβKO ($n = 4$) and control ($n = 7$) mice in different groups than those used in the *in vivo* recordings. Microglia were immunolabelled using rabbit anti-ionized calcium binding adaptor molecule 1 antibody (Iba1) (1/500; WAKO, Cat # 019-1974, RRID: AB_2313566), followed by biotinylated goat anti-rabbit (1:1000, Vector Laboratories, Cat # BA-1000), avidin-biotin complex, and 3,3'-diaminobenzidine (both from Vector Laboratories)

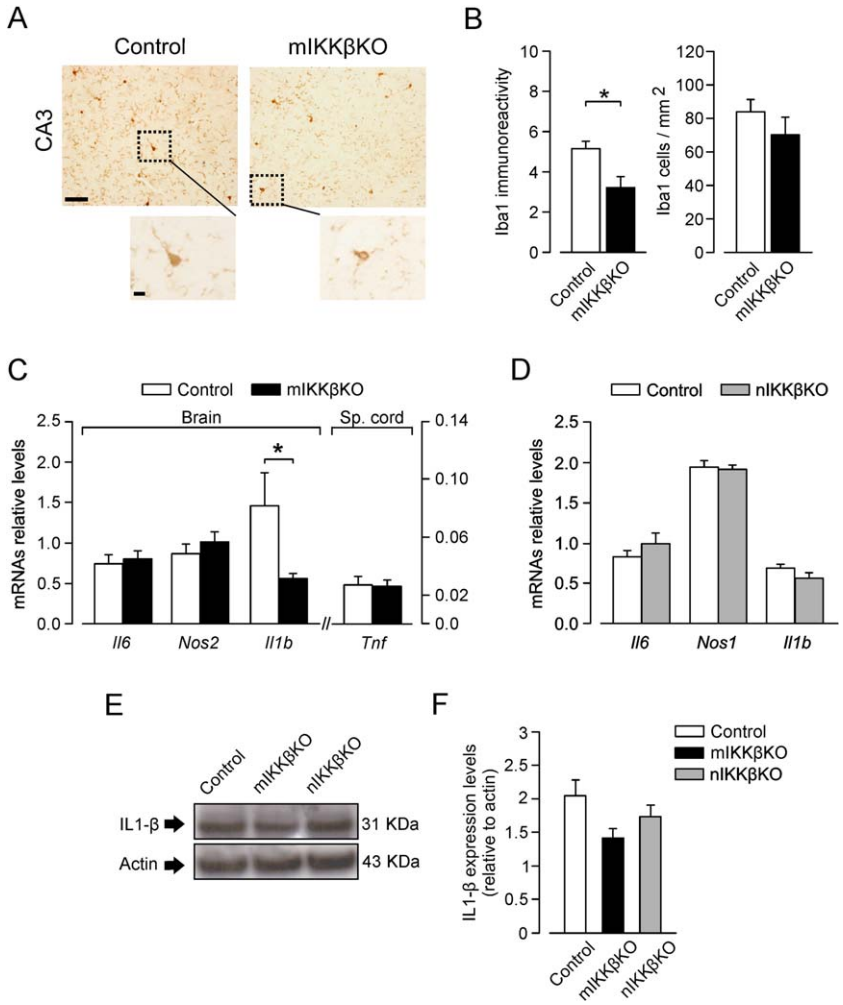

FIGURE 2: mIKKβKO mice show reduced microglial Iba1-immunoreactivity and IL1-β expression in the brain under physiological conditions. (A) Representative photomicrographs showing Iba1-immunoreactive cells in the hippocampal CA3 area (scale bar 50 μm) of control and mIKKβKO mice. Insets show higher magnification of Iba1-immunoreactive cells (scale bar 15 μm). (B) Quantitative analysis of Iba1-immunostaining showing total number of Iba1-positive cells (left) and total area of Iba1-immunoreactivity (right) measured in the CA3 area of control ($n = 7$) and mIKKβKO ($n = 4$) mice (*$P = 0.021$, t test). (C) Levels of *Il6*, *Nos2*, and *Il1b* mRNA in whole brain ($n = 10$ mice per group) and *TNF* in spinal cord (n = 6 per group) from control and IKKβKO mice, relative to *Gapdh*, as measured by quantitative RT-PCR (*$P = 0.038$, Mann-Whitney test). (D) Levels of *Il6*, *Nos1*, and *Il1b* mRNA in whole brain samples from control and nIKKβKO mice ($n = 6$ mice per group), relative to Gapdh, by quantitative RT-PCR. (E) Representative Western blot showing IL1-β protein levels in brains isolated from control, mIKKβKO, and nIKKβKO mice. Actin is shown as a loading control. (F) Quantitative analysis of the immunoblot shown in E ($n = 4$ mice per group). Data are shown as mean ± SEM. [Color figure can be viewed in the online issue, which is available at wileyonlinelibrary.com.]

(Fig. 2A). Antigen retrieval for Iba1 was done in 10 mM EDTA buffer pH 8.5 for 1 h at 95–100°C in a household food steamer. Analysis of the Iba1 staining was performed by using the Image J program for Windows. Total number of Iba1 positive cells, as well as area of Iba1 immunoreactivity were measured in the CA3 hippocampal area (one coronal section per mouse, $n = 7$ control and $n = 4$ mIKKβKO mice). Iba1 positive cells were counted manually per mm^2 of the total CA3 area. Iba1 immunoreactivity was defined as the percentage of positively stained area (in pixels) including microglial cell bodies and processes, relatively to the total CA3 area. It was measured by manually setting a positive staining intensity threshold that was pre-defined in control sections and was used for all the subsequent measurements. Only sections from identical brain regions immunostained in the same experiment were used for comparative analyses and all the photos were taken on the same day using the same parameters.

Data Analysis and Representation

fEPSPs and 1 V rectangular pulses corresponding to lever presses, paired-pulse presentations and HFS were stored digitally on a computer through an analog/digital converter (CED 1401 Plus; Cambridge Electronic Design, Cambridge, England). Data were analyzed offline for quantification of animal performance in instrumental learning and fEPSPs with the Spike 2 (Cambridge Electronics

Design, RRID: rid_000090) program and the video-capture system. Depending on the experiment, 5–15 successive fEPSPs were averaged, and the mean value of the amplitude during the rise-time period (i.e., the period between the initial 10% and the final 10% of the fEPSP) was determined. Computed results were processed for statistical analysis using the Sigma Plot 11.0 package (SigmaPlot, San Jose, CA, USA). Data are represented as mean ± SEM. Acquired data were analyzed with 2-tailed Student's *t* test or the 1-way or 2-way analysis of variance (ANOVA) using days as the repeated measurement followed by a contrast analysis (post-hoc) for further analysis of significant differences.

Results

In the brain, the active form of NF-κB mostly consists of p50/p65 heterodimers, which are sequestered in the cytoplasm by the inhibitor of κB (IκB). NF-κB is activated by multiple stimuli, including basal synaptic transmission, glutamate, kainate, pro-inflammatory cytokines, or depolarization (Kaltschmidt and Kaltschmidt, 2009). Canonical NF-κB (p50/p65) signaling involves activation of NF-κB, mainly following IκB kinase (IKKβ)-mediated phosphorylation and proteasomal degradation of IκB, and release of NF-κB which translocates to the nucleus and activates transcription of target genes (Fig.1A) (Vallabhapurapu and Karin, 2009). In neurons, gene targets include neuroprotective antiapoptotic molecules (Kaltschmidt and Kaltschmidt, 2009) while in cells of myeloid lineage like microglia they include mediators of cell activation and effector function (Hoffmann and Baltimore, 2006) such as IL-1β, a critical microglial-specific regulator of hippocampal-dependent learning and memory processes (Williamson et al., 2011).

Reduced Microglial Area and IL-1β Expression in Brain of Mice With Depletion of IKKβ in Cells of Myeloid Lineage

Recent studies show that microglia play an important role in controlling neuronal activity under normal physiological conditions. To investigate the role of microglia in synaptic plasticity and cognitive function, we generated mice in which IKKβ is selectively depleted in cells of myeloid origin. To do this, we crossed $IKK\beta^{F/F}$ mice (Park et al., 2002; Li et al., 2003) with transgenic mice expressing Cre recombinase under the control of the CD11b promoter (Fig. 1B).

mIKKβKO mice showed normal development, reproduced normally and histology showed no obvious abnormalities in brain structure, including the hippocampus, compared with ($IKK\beta^{F/F}$) controls (Fig. 1C). Cell-specific depletion of IKKβ in myeloid lineage cells of mIKKβKO mice was confirmed in Western blots of total protein lysates from cultures of peritoneal macrophages, microglia and, as a control, astrocytes (Fig. 1D). Quantitative analysis showed that depletion of IKKβ protein levels in mIKKβKO macrophages was approximately 44% and in mIKKβKO microglia was 37% compared with controls, while levels in astrocytes were not reduced (Fig. 1E). These findings are consistent with a previous study using our CD11b-Cre transgenic mice, which showed 50% Cre-dependent depletion of a loxP-flanked transgene in peritoneal macrophages and 25% depletion in cultures of primary microglia (Boillée et al., 2006). To investigate the functional impact of microglial IKKβ depletion, we analyzed the levels of phosphorylated IκB in microglial cells isolated from mIKKβKO and control mice and incubated in the absence or presence of LPS (10 μg/mL, 30 min) by Western blot. Levels of phosphorylated IκB were increased by LPS in microglia from both mouse strains (Fig. 1F, G, $^{**}P = 0.005$, *t* test in controls), but LPS-treated cells from mIKKβKO mice showed reduced induction of phosphorylated IκB compared with those from control mice confirming that IKKβ activity is reduced in mIKKβKO microglia.

To further investigate the cell-specificity of IKKβ targeting in microglia, we compared the effects of mIKKβKO mice with mice in which the conditional IKKβ allele was depleted selectively in CamkII-expressing neurons (nIKKβKO). A basic characterization of nIKKβKO mice has been previously described in which differences in the regional distribution of IKKβ depletion in the brain was apparent (Emmanouil et al., 2009). Based on this previous data we estimate that IKKβ depletion in cortical neuron cultures from nIKKβKO mice is approximately 90%. Here we additionally measured IKKβ depletion in different brain regions of nIKKβKO mice by Western blot (Fig. 1H). Production of IKKβ was significantly reduced in whole brain (46% depletion) and cortex (83% depletion) of nIKKβKO compared with controls, and reduction was also noted in the hippocampus (44% depletion) although this did not reach statistical significance (Fig. 1I, $^{*}P = 0.045$, $^{***}P = 0.001$, *t* test). Production of IKKβ in the cerebellum was not altered. We also checked whether depletion of IKKβ in mice altered the density of dendritic spines in hippocampal neurons. Double immunofluorescence staining of cultured hippocampal neurons isolated from nIKKβKO, mIKKβKO, and control mice using antibodies to the post-synaptic protein PSD95 and tubulin (beta III isoform) as a marker for neuronal cytoskeleton (see Supp. Info. Materials and Methods), showed that spine morphology (Supp. Info. Fig. 3A) and spine density (Supp. Info. Fig. 3B) were similar in neurons from the three mouse strains.

We next compared the morphology of microglia in mIKKβKO mice and controls under basal conditions. We performed immunohistochemistry on hippocampal sections from naïve mice using antibody to Iba1, a calcium-binding protein that is expressed specifically in microglia and plays an important role in their activation (Imai and Kohsaka, 2002) (Fig. 2A). The number of Iba1-immunoreactive cells in the

hippocampal CA3 region was not significantly different between mIKKβKO and control mice but the area covered was less in mIKKβKO (Fig. 2B, $^*P = 0.021$, *t* test), reflecting reduced Iba1-immunoreactivity and therefore possibly reduced microglial cell size.

To evaluate the impact of microglial IKKβ depletion on the expression of NF-κB target genes, we analyzed the expression of genes encoding IL-1β, IL-6, and inducible NOS, which are well-studied targets of NF-κB signaling (Cho et al., 2008), in mIKKβKO and control CNS tissues by qRT-PCR. Expression of *Il1b*, but not *Il6* or *Nos2*, was markedly reduced in the brain of mIKKβKO mice compared with controls (Fig. 2C, $^*P = 0.038$, Mann-Whitney test). The expression of *Tnf*, as measured in spinal cord tissues, was equal in mIKKβKO and control mice (Fig. 2C). In contrast to mIKKβKO mice, the expression of *Il1b*, *Il6*, and *Nos1*, which encodes neuronal NOS, in nIKKβKO brain was equal to controls (Fig. 2D), suggesting that neuronal IKKβ does not participate in regulating these cytokines under resting conditions. We also measured the production of IL-1β in mIKKβKO, nIKKβKO, and control CNS tissues by Western blot. Production of IL-1β in mIKKβKO brain was reduced compared with control and nIKKβKO brain, although the levels under physiological conditions were low in all strains and differences did not reach statistical significance (Fig. 2E, F). In conclusion, microglia that are deficient in IKKβ, and therefore also NF-κB activity, show reduced Iba1-immunoreactivity and express lower levels of IL-1β in the normal brain.

Enhanced Short-Term Synaptic Plasticity in the Hippocampus of Freely Moving mIKKβKO Mice

We measured the functional properties of the CA3-CA1 synapse *in vivo*, by stimulating the Schaffer collateral pathway in freely moving mIKKβKO, nIKKβKO and control mice (Fig. 3A). To measure synaptic integrity in this pathway, electrophysiological recordings were taken from mice in which the stimulating and recording electrodes had been permanently implanted in the CA3 (Schaffer collaterals) and ipsilateral CA1 areas of the right hippocampus, respectively (Fig. 3A, B). Animals were allowed to recover at least 7 days after the implantation of the electrodes and before the electrophysiology recordings. First, we measured synaptic transmission (input-output test) by recording changes in fEPSP amplitudes evoked in the pyramidal CA1 area by paired-pulse (40 ms of interpulse interval) stimulation of increasing intensity (0.02–0.4 mA, in 0.02 mA steps). In control and nIKKβKO mice, fEPSP amplitude evoked by the first and second pulses increased steadily with current strength showing a typical sigmoid curve (Figs. 3C and 4A). In mIKKβKO mice fEPSP amplitude evoked by first pulse was similar to controls but the synaptic response from the second pulse tended to be higher at lower stimulation intensities (Fig. 3C, gray shaded area, Fig. 4A) and lower at higher stimulation intensities, resulting in a flater curve compared with control and nIKKβKO mice. Although these differences were not statistically significant (1st pulse: $F_{(1,9,36)} = 0.744$, $P = 0.568$; 2nd pulse: $F_{(1,9,36)} = 0.725$, $P = 0.581$), these data give a first indication that mIKKβKO mice tend to show altered synaptic properties.

We next evaluated presynaptic function at the hippocampal CA3-CA1 synapse using the paired-pulse facilitation (PPF) test, a form of short-term plasticity. Here, presynaptic neurons receive a pair of stimuli in rapid succession causing a transient accumulation of calcium in presynaptic nerve terminals. The increase in the ratio of the second/first fEPSP response (facilitation) at short (<60 ms) intervals reflects mainly the increase in presynaptic calcium which in turn increases the probability of neurotransmitter release. We stimulated mIKKβKO, nIKKβKO, and control mice with paired pulses using a wide range of interstimulus intervals (10–500 ms). All groups of mice presented a significant increase in response to the second pulse at the short time intervals (10, 20, and 40 ms) with the response in mIKKβKO, not nIKKβKO mice, being significantly higher than that in controls at the 40 ms interval ($^*P = 0.043$, Holm-Sidak test; Figs. 3D and 4B). This result demonstrates that mIKKβKO mice presented a higher facilitation to the second pulse during the paired-pulse test as compared with control mice, indicating lower neurotransmitter release probability at the synapses of mIKKβKO mice. It could also reflect possible impairment in glutamate uptake mechanisms, which are regulated by glial cells including microglia (Schafer et al., 2013). For this reason, we measured the production of glutamate transporter-1 (GLT-1/EAAT2), which is selectively produced by microglia (Nakajima et al., 2001) and is involved in the removal of glutamate from the extracellular space, in protein lysates from microglial cell cultures. No differences in the constitutive levels of GLT-1/EAAT2 production were detected between mIKKβKO and control microglial cells (Supp. Info. Fig. 4), indicating that extracellular glutamate uptake might not be altered by IKKβ depletion in microglial cells. Overall, our results show that microglia act to regulate neuronal excitability as measured in the Schaffer collateral pathway of the hippocampus, through mechanisms such as control of presynaptic neurotransmitter release, and this effect is mediated by IKKβ.

Freely Moving mIKKβKO and nIKKβKO Mice Show Different Impairments in Long-Term Potentiation

To further investigate the role of microglial IKKβ in synaptic plasticity, we induced LTP by high frequency stimulation (HFS) of the hippocampal Schaffer collateral pathway and

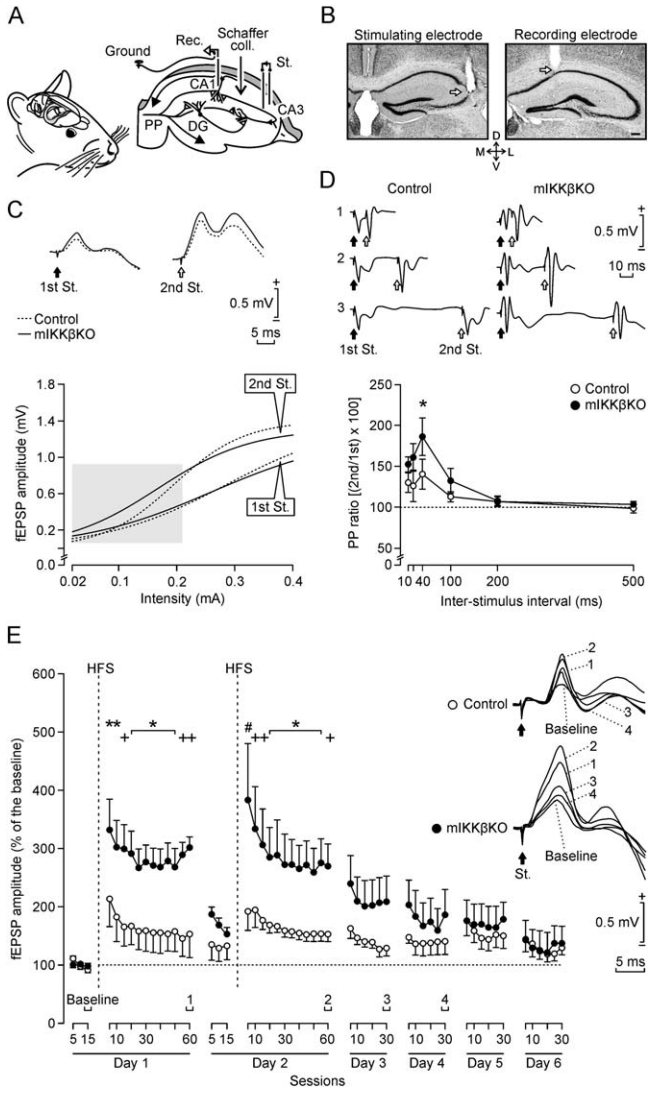

FIGURE 3: Input/output curves, paired-pulse facilitation and LTP evoked at the CA3-CA1 synapse with HFS under alert behaving conditions showed increased PPF and higher LTP in mIKKβKO mice. (A) Bipolar stimulating electrodes (St.) were chronically implanted in the CA3 area of the right hippocampus to activate the Schaffer collateral/commissural pathway (Schaffer coll.). Recording electrodes (Rec.) were implanted in the ipsilateral CA1 area. (B) Photomicrographs illustrating the location (white arrows) of the stimulating and recording sites, in coronal hippocampal sections. Scale bar, 200 μm. Abbreviations: D, dorsal; L, lateral; M, medial; V, ventral. (C) Regression lines illustrating input/output curves evoked at the CA3-CA1 synapse of control and mIKKβKO ($n = 10$ per group) mice. Paired pulses (40 ms of interstimulus interval) were delivered at increasing intensities in 20 μA steps. Dotted and unbroken lines represent the sigmoid regression lines evoked from the mean value computed from five stimulus presentations of the 1st pulse ($R^2 = 0.9904$, $P = 0.0096$) and 2nd pulse ($R^2 = 0.9988$, $P = 0.0012$) in control mice and of the 1st pulse ($R^2 = 0.9983$, $P = 0.0017$) and 2nd pulse ($R^2 = 0.9849$, $P = 0.0151$) in knockouts, respectively. Representative examples of fEPSP recordings (0.2 mA) of control (dotted line) and mIKKβKO (unbroken line) mice are also illustrated. (D) Paired-pulse facilitation was evoked in control and mIKKβKO mice ($n = 10$ per group) by stimulating Schaffer collaterals with a fixed current (30-40% of the amount required to evoke a saturating response). Averaged (5 times) fEPSPs paired traces were collected at interstimulus intervals of 10, 20, 40, 100, 200, and 500 ms. Data shown are mean ± SEM amplitudes of the second fEPSP expressed as the percentage of the first [(second/first) × 100] for each of the six interstimulus intervals used in this test (PP ratio) ($F_{(1,9,45)} = 1.319$, $^{*}P = 0.043$, Holm-Sidak test). Averaged fEPSP recordings collected from representative control and mIKKβKO mice after paired-pulse stimulations (arrows) with 10 (1), 40 (2), and 100 (3) ms interstimulus intervals are also illustrated. (E) Graph illustrating the time course of changes in fEPSP amplitudes (LTP) after HFS of the Schaffer collaterals in control and mIKKβKO ($n = 8$ per group) mice. The HFS train was presented after 15 min of baseline recordings on 2 consecutive days, at the time indicated by the vertical dashed lines. The fEPSP amplitudes are expressed as a percentage of the baseline (Day 1, before HFS) amplitude (100%) in each group. Illustrated data were collected up to 60 min after HFS during the first (Day 1) and second (Day 2) days, and for 30 min on Days 3, 4, 5, and 6 after the first HFS. The two groups presented a significant increase in fEPSP amplitude after HFS compared with baseline recordings. In addition, values collected from mIKKβKO mice were significantly larger ($F_{(1,7,371)} = 2.313$, $^{***}P < 0.001$) than those from controls at the indicated times ($^{*}P < 0.05$; $^{+}P < 0.01$; $^{\#}P < 0.001$). Representative fEPSPs recorded in the CA1 area from control (up) and mIKKβKO (down) mice before (baseline) and 1, 2, 3, and 4 days after HFS of Schaffer collaterals are also shown. Data are shown as mean ± SEM and statistical analysis by two-way ANOVA, repeated measures.

compared the evolution of fEPSPs evoked at the CA3-CA1 synapse in freely moving mIKKβKO, nIKKβKO, and control mice (Figs. 3E and 4C). HFS was delivered as five trains (200 Hz, 100 ms) of pulses at a rate of 1/s. Baseline recordings (15 min) and HFS sessions were performed on days 1 and 2 using the same stimulation parameters (Figs. 3E and 4C) and LTP was measured as the amplitude of fEPSPs evoked by each session of HFS followed by 1 h of postHFS recordings. Subsequently, additional daily recordings of 30 min each were taken up to day 6. Normalization of the results from the entire *in vivo* LTP protocol was performed using day 1 baseline recordings for each mouse. All mouse strains showed significant LTP responses on day 1. mIKKβKO mice showed a significantly larger response to HFS ($F_{(1,7,371,)} = 2.313$; $^{***}P < 0.001$, two-way repeated measures, ANOVA) than controls on both days 1 and 2, with fEPSP amplitude returning to control levels between the two HFS sessions (Fig. 3E). In contrast, nIKKβKO mice showed an equal response to controls on day 1, but failed to induce LTP following the second HFS on day 2 (Fig. 4C, $F_{(1,7,371)} = 2.318$; $^{***}P < 0.001$, two-way repeated measures, ANOVA).

These results demonstrate that microglia and neurons are independently important for modulating LTP following HFS of Schaffer collaterals through the action of IKKβ, but in different ways. Microglial IKKβ is involved in regulating the excitability of neurons in response to HFS without affecting their ability to generate LTP. This is further

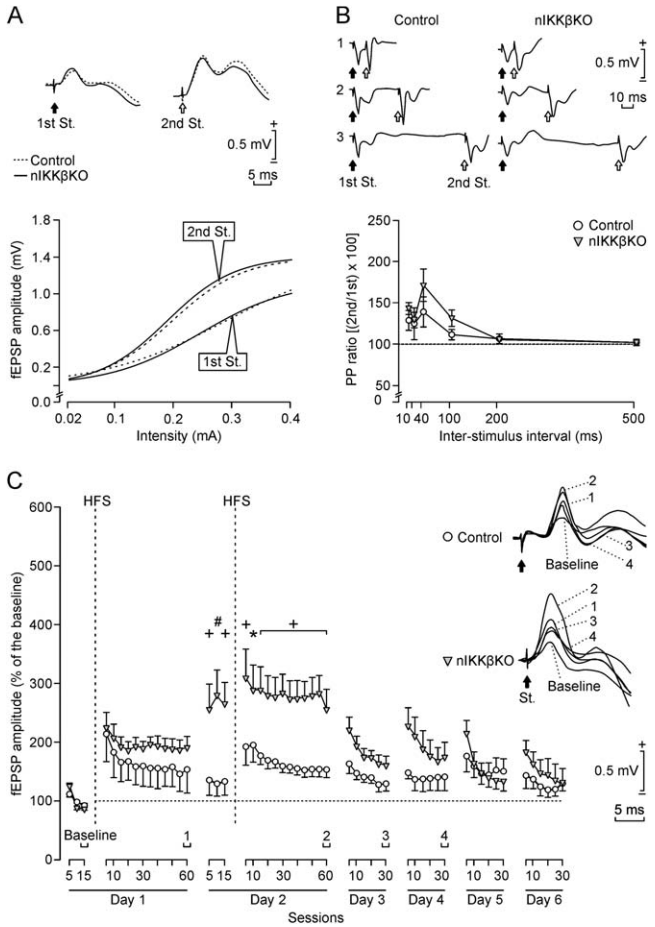

FIGURE 4: Input/output curves, paired-pulse facilitation and LTP evoked at the CA3-CA1 synapse with HFS under alert behaving conditions showed normal synaptic transmission but impairment in LTP induction at later phases in nIKKβKO mice. (A) Regression lines illustrating input/output curves evoked at the CA3-CA1 synapse of control and nIKKβKO ($n = 10$ per group) mice. Paired pulses (40 ms of interstimulus interval) were delivered at increasing intensities in 20 μA steps. Dotted and unbroken lines represent the sigmoid regression lines evoked from the mean value computed from five stimulus presentations of the 1st pulse ($R^2 = 0.9904$, $P = 0.0096$) and 2nd pulse ($R^2 = 0.9988$, $P = 0.0012$) in control mice and of the 1st pulse ($R^2 = 0.9988$, $P = 0.0012$) and 2nd pulse ($R^2 = 0.9991$, $P = 0.0005$) in knockouts, respectively. Representative examples of fEPSP recordings (0.2 mA) of control (dotted line) and nIKKβKO (unbroken line) mice are also illustrated. (B) Paired-pulse facilitation was evoked in control and nIKKβKO mice ($n = 10$ per group) by stimulating Schaffer collaterals with a fixed current (30% - 40% of the amount required to evoke a saturating response). Averaged (5 times) fEPSPs paired traces were collected at interstimulus intervals of 10, 20, 40, 100, 200, and 500 ms. Data shown are mean ± SEM amplitudes of the second fEPSP expressed as the percentage of the first [(second/first) × 100] for each of the 6 interstimulus intervals used in this test (PP ratio). Averaged fEPSP recordings collected from representative control and nIKKβKO mice after paired-pulse stimulations (arrows) with 10 (1), 40 (2), and 100 (3) ms interstimulus intervals are also illustrated. (C) Graph illustrating the time course of changes in fEPSP amplitudes after HFS of the Schaffer collaterals in control and nIKKβKO ($n = 8$ per group) mice. The HFS train was presented after 15 min of baseline recordings on 2 consecutive days, at the time indicated by the vertical dashed lines. The fEPSPs amplitudes are expressed as a percentage of the baseline (Day 1, before HFS) amplitude (100%) in each group. Illustrated data were collected up to 60 min after HFS during the first (Day 1) and second (Day 2) days, and for 30 min on Days 3, 4, 5, and 6 after the first HFS. The two groups presented a significant increase in fEPSP amplitude after the 1st but not after the 2nd HFS compared with baseline recordings. In addition, values collected from nIKKβKO mice were significantly larger ($F_{(1,7,371)} = 2.318$, $^{***}P < 0.001$) than those from controls at the indicated times ($^{*}P < 0.05$; $^{+}P < 0.01$; $^{\#}P < 0.001$). Representative fEPSPs recorded in the CA1 area from control (up) and nIKKβKO (down) mice before (baseline) and 1, 2, 3, and 4 days after HFS of Schaffer collaterals are also shown. Data are shown as mean ± SEM and statistical analysis by two-way ANOVA, repeated measures.

supported by the finding that hippocampal neurons in mIKKβKO mice showed higher electrical activity in response to peripheral administration of low doses of kainic acid compared with those in nIKKβKO and control mice (Supp. Info. Materials and Methods and Fig. 5). In contrast, neuronal IKKβ is not required for the induction of LTP by the first HFS but is critical for LTP induction by the second HFS, suggesting that neuronal NF-κB activity is required for LTP induction at a later phase which is known to be dependent on gene transcription and thought to correspond to the initial stages of memory consolidation (Citri and Malenka, 2008).

Normal Motor Learning but Increased Anxiety and Differential Disturbances in Short-Term and Long-Term Fear Memory in mIKKβKO and nIKKβKO Mice, Respectively

To investigate whether functional changes in brains of mIKKβKO and nIKKβKO mice, such as the altered hippocampal electrical activity described above, are paralleled by altered learning and memory processes we compared the performance of mIKKβKO and nIKKβKO mice with controls using standard behavioral tests. Coordination and the ability to acquire motor skill were tested using an accelerating rotarod test. mIKKβKO mice showed better baseline motor performance than controls on the first acquisition day ($^{*}P = 0.028$, Mann-Whitney test) and thereafter showed similar performance (Fig. 5A). nIKKβKO mice showed equivalent performance to controls at all time points (Fig. 5B).

In an open field arena, a measure of exploratory behavior and of anxiety evoked by open spaces, mIKKβKO mice showed less spontaneous locomotor activity than controls early in the test, as measured by the amount of distance traveled ($^{***}P < 0.001$, Mann-Whitney test; Fig. 5C, left) and increased anxiety as shown by less time spent in the center of the arena ($^{**}P < 0.01$, Mann-Whitney test; Fig. 5C, right). In this test, nIKKβKO mice showed

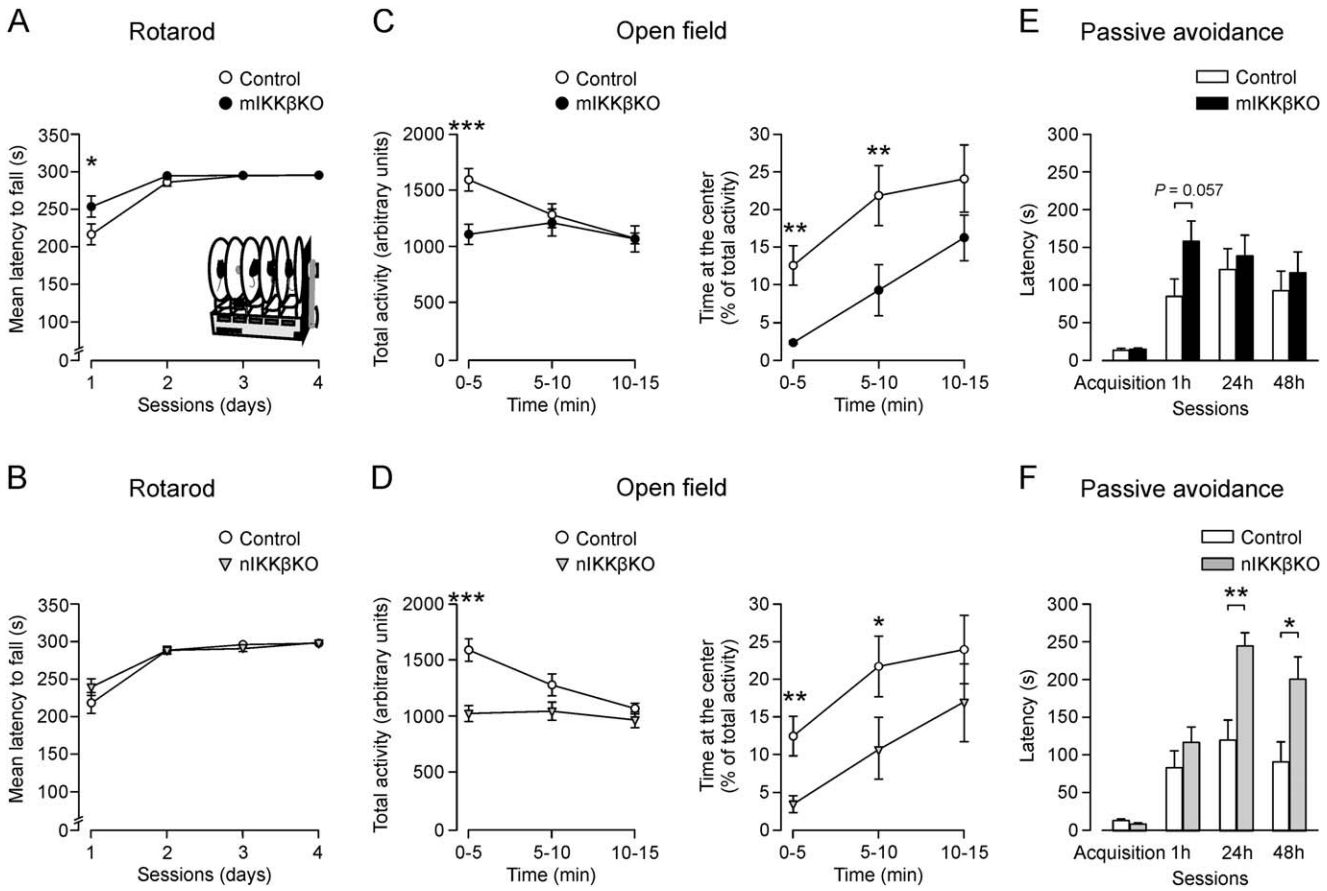

FIGURE 5: Performance in rotarod, open field, and passive avoidance tasks showed increased anxiety levels in both mIKKβKO and nIKKβKO mice but differential increases in short-term and long-term contextual fear memory, respectively. (A, B) Rotarod test: Mean latency to fall (s) refers to the total time (average of two trials per day) that each mouse spent on the rod before falling. Comparison of performance of mIKKβKO (A) mice and nIKKβKO (B) mice with controls ($n = 14$ per group) (*$P = 0.028$, t test). (C,D) Open field task: Horizontal locomotor activity (total activity, left graph) and center time exploration (right graph) were measured for three consecutive periods of five min each. (C) mIKKβKO mice presented less horizontal locomotor activity (*$P < 0.001$, t test) and center time exploration during the first (0–5 min, **$P = 0.004$, t test) and second time points (5–10 min, **$P = 0.008$, t test) than controls ($n = 14$ per group). (D) nIKKβKO mice presented less horizontal locomotor activity (***, $P < 0.001$, t test) and center time exploration during the first (0–5 min, *$P = 0.014$, Mann-Whitney test) and second time points (5–10 min, *$P = 0.02$, Mann-Whitney test) than controls ($n = 14$ per group). (E, F) Passive avoidance task: Latency refers to the time mice spent in the illuminated area before enterance to the dark compartment, which was paired with a foot shock, on the acquisition day. (E) Comparison of performance in mIKKβKO and control mice ($n = 13$ per group) ($P = 0.057$, Mann-Whitney test). (F) Comparison of performance in nIKKβKO and control mice ($n = 13$ per group) (**$P = 0.003$; *$P = 0.012$, t test). Data are shown as mean ± SEM.**

a similar pattern of behavior as mIKKβKO mice (Fig. 5D, ***$P < 0.001$; *$P < 0.05$, Mann-Whitney test).

We next measured the performance of mIKKβKO and nIKKβKO mice in a passive avoidance task which is used to study learning and memory for stress stimuli and involves mainly dorsal hippocampus and amygdala (Phillips and LeDoux, 1992; Baarendse et al., 2008). Animals were trained in a two-chamber (dark/light) apparatus to avoid the dark chamber because it was associated with a footshock of 0.6 mA during the acquisition phase. Animals were then measured for extinction of the fear memory, which was induced by repetition of the experimental procedure in the absence of the footshock over a 48 h period. mIKKβKO and control mice showed equivalent responses during acquisition, but mIKKβKO showed a transiently increased reluctance to enter the dark chamber 1 h afterward ($P = 0.057$, Mann-Whitney test) (Fig. 5E). nIKKβKO and control mice also showed similar responses during acquisition, but nIKKβKO mice showed markedly increased fear memory at the later 24 and 48 h post-acquisition time points (Fig. 5F, *$P = 0.012$, t test; **$P = 0.003$, Mann-Whitney test). Collectively, these findings show that microglia and neurons both independently contribute to mouse behavior through the production of IKKβ, but in distinct ways. Specifically, motor learning ability was normal while anxiety in an open field arena was similarly increased in mIKKβKO and nIKKβKO mice. Cell-specific differences were revealed in the contextual fear conditioning paradigm where mIKKβKO mice showed transiently increased short-term fear

memory compared with controls, while nIKKβKO mice showed increased long-term fear memory that might involve impairment of memory extinction. Combined, the observed impairments in synaptic plasticity and contextual fear memory, which are known to share common molecular mechanisms (Schafe et al., 1999), show that microglial IKKβ is important for the homeostatic regulation of hippocampal neuronal activity while neuronal IKKβ is critical for long-term functional processes that probably involve the activation of NF-κB and induction of gene transcription.

Microglia and Neurons Independently Contribute, Through IKKβ, to Associative Learning in Instrumental Conditioning

To investigate whether microglia contribute, through production of IKKβ, to associative learning, we next tested the performance of mIKKβKO mice in instrumental conditioning tasks as previously described (Hasan et al., 2013). This paradigm measures learning and memory, as well as behavioral modifications that take place during the performance of appetitive and consummatory behaviors that are driven by reward (food pellet). It also allows direct recording of fEPSP evoked at the CA3-CA1 synapse which has previously been shown to contribute to these behaviors in wild type C57BL/6 mice (Jurado-Parras et al., 2013) (see next section).

We compared mIKKβKO and nIKKβKO mice with controls in a learning paradigm, herein referred to as Instrumental test I, for their ability to learn a conditioning task in which they first had to press a lever to obtain a food reward in a 1:1 fixed-ratio schedule (Fig. 6A, B, top). Daily, 20 min conditioning sessions were performed until mice reached a set criterion level of 20-lever presses/session on 2 consecutive days. All three groups of mice progressively improved their performance and reached the criterion level but mIKKβKO mice (Fig. 6C, D), not nIKKβKO mice (Fig. 6F, G), showed a significant delay compared with controls, acquiring the instrumental conditioning task in 6.69 ± 0.33 days compared with 5.27 ± 0.18 in controls ($^{**}P = 0.003$, t test) (Fig. 7E).

Animals that had reached the criterion level were subsequently trained in a more complex situation where mice had to modify their learned behavior to incorporate sensory information. Here, animals received the food reward (again in a 1:1 fixed-ratio schedule) only when the lever press was performed during a light period of 20 s. Lever presses in the dark were punished by an additional random 1–10 s delay in appearance of the next light period (Fig. 6B, bottom). All three groups of mice reached point zero, defined as the point when lever-presses in light and dark periods were equal, without significant difference around day 8 (data not shown). Since individual mice differed slightly in reaching point zero, we analyzed the data after synchronization of mice according to their own point zero, a point that was labeled after as Day 0. After that point, the control mice continued to show progressively improved performance while mice in the KO groups did not, and significant differences were observed for both mIKKβKO (Fig. 6I) ($^{**}P = 0.002$; $^{*}P = 0.038$, Holm-Sidak method) and nIKKβKO (Fig. 6J) ($^{**}P = 0.005$, Holm-Sidak method) groups compared with controls. These results demonstrate that microglial IKKβ is essential for efficient instrumental conditioning performance at all levels of the learning process while neuronal IKKβ contributes to successful performance of tasks that require a higher level of cognitive ability.

IKKβ is Independently Required in Microglia and Neurons for Behavior Modification and Increase of Hippocampal Synaptic Strength During Appetitive, Not Consummatory, Behavior

To further investigate the effect of microglial and neuronal IKKβ on associative learning and to directly measure synaptic strength across the hippocampal CA3-CA1 synapse during selected cognitive processes in the behaving mice, we carried out a second set of learning experiments, herein referred to as Instrumental test II (Fig. 7A), using mice with permanently implanted electrodes (Fig. 3A, B). Mice from mIKKβKO, nIKKβKO and control groups were placed in individual Skinner boxes and were able to move freely while connected to the recording wires. Performance parameters and changes in activity-dependent strengths of the CA3-CA1 synapse were measured during acquisition of the 1:1 fixed-ratio schedule lever-press/food-reward task described above. For measuring the synaptic strength, a single 100 μs, square, biphasic pulse was presented at the Schaffer collaterals, and evoked fEPSPs were recorded in the ipsilateral pyramidal CA1 layer (Fig. 3A, B). The stimulus was presented during the performance of two selected behaviors: appetitive behavior, "going-to-lever" and consummatory, "going-to-feeder," i.e., crossing a photoelectric cell positioned 5 cm in front of the lever or feeder, respectively (Fig. 7A). The stimulus was repeated daily from day 1 of the experiment until 3 days after a criterion level, set at the first day of two successive sessions with a minimum of 20 lever presses/session (day 0), was reached by each animal. Synaptic strength was measured as fEPSP amplitudes and collected prior to (pre-session) and during the two different behaviors and was either normalized independently for each animal against the pre-session value on day 1 of the experiment (Fig. 7B) or expressed as a ratio of fEPSPs going-to-lever relative to going-to-feeder during the daily experimental session (Fig. 7C).

Pre-session fEPSP amplitudes remained stable throughout the training procedure in both control and nIKKβKO mice (Fig. 7B). In contrast, fEPSP amplitudes were higher in mIKKβKO mice than in controls (Fig. 7B, $F_{(1,5,30)} = 2.738$, $^{*}P = 0.03$, two way ANOVA, repeated measures) and also

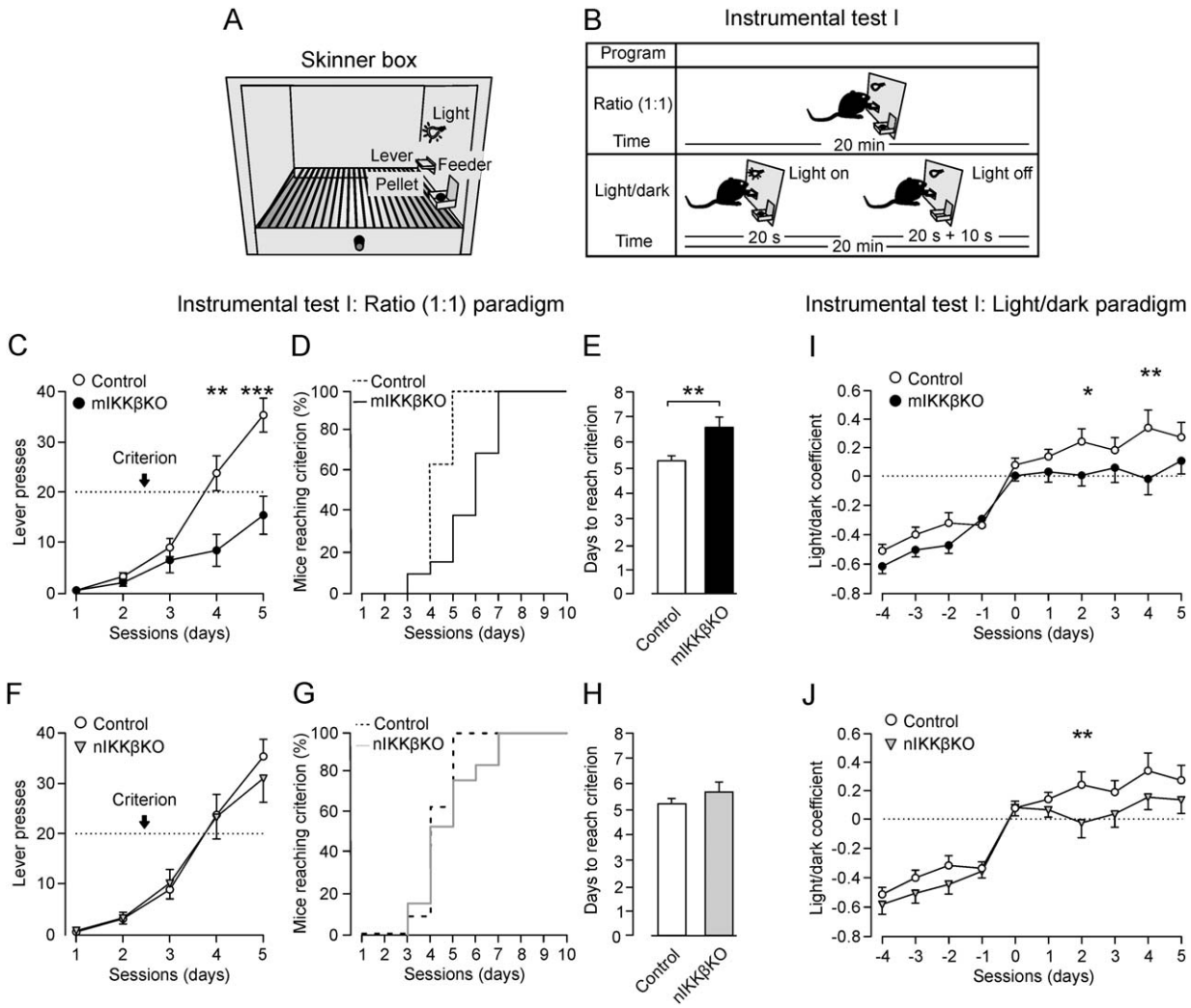

FIGURE 6: Inability of mIKKβKO and nIKKβKO mice to incorporate sensory information during instrumental conditioning. (A) Diagram of the Skinner box used in Instrumental test I to train mice to press a lever for pellet reward in the feeder. (B) Schematic representation of the Instrumental test I to train mice with two sequential programs of increasing difficulty. First, a fixed-ratio (1:1) schedule where mice were required to reach a criterion level of 20 pellets/20 min session for 2 consecutive days (top) before proceeding to the second program. Second, a light/dark paradigm (bottom), where lever pressing was only reinforced by a food pellet reward when the light was on. Lever presses during the dark period delayed the start of the next lighted period for an additional 10 s. (C) Lever presses by mIKKβKO and control ($n = 13$ per group) mice in order to reach the criterion level (dotted line). Performance during the first five training days is illustrated. Differences between groups are indicated ($F_{(1,12,48)} = 15.580$, $^{***}P < 0.001$). (D) Cumulative percentage of mice shown in (C) reaching the criterion across the successive sessions. (E) Days required for mice shown in (C) to reach criterion ($^{**}P = 0.003$, *t* test). (F–H) Performance of nIKKβKO mice in 1:1 fixed-ratio schedule task, compared with controls. (F) Lever presses by nIKKβKO and control ($n = 13$ per group) mice in order to reach the criterion level (dotted line). Performance (lever presses) during the first five training days is illustrated. (G) Cumulative percentage of mice shown in (F) reaching criterion across the successive sessions. (H) Days required for mice shown in (F) to reach criterion. (I, J) In the second task, mice were presented with another 1:1 fixed-ratio schedule in which the food reward was associated with light (light/dark paradigm). Point 0 was defined as the day the mice pressed the lever equally during light and dark periods. The light/dark coefficient was calculated as follows: (number of lever presses during the light period − number of lever presses during the dark period)/total number of lever presses. (I) Performance of mIKKβKO and control ($n = 10$ mice per group) groups after synchronizing individual mice according to the day they reached point 0, revealed differences after reaching point 0 at the indicated time points ($F_{(1,9,81)} = 1.096$, $^{*}P = 0.038$, $^{**}P = 0.002$). (J) Performance of nIKKβKO and control ($n = 10$ mice per group) groups after synchronizing individual mice according to the day they reached point 0, revealed differences after reaching point 0 at the indicated time points ($F_{(1,9,81)} = 0.975$, $^{**}P = 0.005$). Data are shown as mean ± SEM and statistical analysis was made by two way ANOVA, repeated measures (C, I, J) and *t* test (E).

increased during the learning process (Fig. 7B, d-3 vs. d0: $^{\#\#}P < 0.001$, Holm Sidak method). These results suggest a higher neuronal responsiveness to a familiar context in mIKKβKO mice. To evaluate hippocampal function associated with appetitive and consummatory behaviors we next measured the ratio between fEPSP amplitudes during going-to-lever and going-to-feeder, respectively. It was recently shown that synaptic strength at this synapse in C57BL/6

mice is specifically increased during the performance of appetitive but not consummatory behaviors (Jurado-Parras et al., 2013). Consistent with this, in control mice the appetitive/consummatory ratio increased in parallel with learning (Fig. 7C). However, neither nIKKβKO nor mIKKβKO mice showed this increase (Fig. 7C) indicating disruption of normal hippocampal function specifically during the performance of appetitive behavior.

To understand whether altered hippocampal fEPSP activity, as measured throughout the acquisition of this instrumental task, also reflects alterations in performance we next compared behavioral parameters between the three strains. When individual mice were synchronized according to day 0, the overall performance of the three strains, as measured by total lever presses, was equivalent (Fig. 7D). However, the different strains showed marked differences in the performance of individual behaviors. First, mIKKβKO mice spent significantly more time between releasing the lever and visiting the feeder than control or nIKKβKO mice when measured after the criterion was passed (Fig. 7E, $^{**}P = 0.008$; $^{*}P = 0.032$, Mann-Whitney test), suggesting that even though both knockout mice have learned to associate their action with the outcome to the same level as the controls, the navigation strategy of mIKKβKO and to a lesser extent of nIKKβKO mice was disturbed. This result is consistent with the observed disturbances in hippocampal fEPSPs in both groups, given the critical role of the hippocampus as a cognitive map and of hippocampal place cells in integration of signals deriving from translational and directional components of movements (Whishaw et al., 1997).

We next investigated the individual going-to-lever (appetitive) and going-to-feeder (consummatory) behaviors. As expected, performance improved over time in control mice as shown by increased visits to the lever (Fig. 7F), decreased visits to the feeder (Fig. 7G) and a decreased error index (going-to-feeder/going-to-lever) (Fig. 7H) after the criterion was reached (day 0). However, although both nIKKβKO and mIKKβKO mice showed reduced visits to the feeder in a similar way to the controls (Fig. 7G), the number of visits to the lever was not correspondingly increased (Fig. 7F). Further analysis showed that the error index was decreased in nIKKβKO and control, but not mIKKβKO mice. Collectively, we show that microglia and neurons are independently and selectively important for proper hippocampal synaptic function during the performance of appetitive, not consummatory behavior in associative learning, and that these effects are dependent on cell-autonomous IKKβ function.

Discussion

In this study, we directly investigated the functions of microglial and neuronal IKKβ in the brain during synaptic plasticity and associative learning by combining cell-specific conditional gene targeting for IKKβ, the main activating kinase in the canonical NF-κB signaling pathway (Vallabhapurapu and Karin, 2009), with recording of hippocampal synaptic activity in behaving animals. We show that microglial and neuronal IKKβ differentially contribute to neuronal function and cognitive processes. Microglial IKKβ is required for regulating short-term and long-term forms of hippocampal synaptic plasticity and the magnitude of fear memory, whereas neuronal IKKβ is required for long-term effects such as the maintenance of synaptic plasticity and the timely extinction of fear memory. We also show that both microglial and neuronal IKKβ contribute to the modification of hippocampus-dependent behaviors in passive avoidance and instrumental conditioning paradigms. Besides predictable requirements for IKKβ in neuronal function, our data identify a novel and unexpected role for microglial IKKβ in the homeostatic regulation of hippocampal synaptic plasticity and the activity of neuronal circuits involved in associative learning and modulation of fear memory.

Microglial IKKβ was found to be necessary for downregulating hippocampal neuronal excitability in models of LTP, kainic acid sensitivity, and instrumental learning, and this effect might provide a functional correlate for recent findings concerning the behavior of these cells in the healthy brain *in vivo*. Microglia are highly dynamic cells (Davalos et al., 2005; Nimmerjahn et al., 2005) that form direct contacts with neuronal synapses in an activity-dependent manner (Wake et al., 2009; Tremblay et al., 2010). The functional significance of such microglia-neuron interactions was only recently indicated by studies in larval zebrafish where microglia reduced spontaneous and visually evoked activities of contacted neurons in the optic tectum (Li et al., 2012). Consistent with a similar function in mammals, depletion of microglia from mouse hippocampal brain slices with clodronated liposomes increased the frequency of excitatory postsynaptic currents and, conversely, microglia decreased synaptic activity in cultures of hippocampal neurons (Ji et al., 2013). A key role for microglia in the control of synaptic plasticity in the hippocampus has already been indicated by studies with gene knockout mice. Mice deficient in the microglia inhibitory mediators, CX3CR1 (fractalkine) (Rogers et al., 2011), and CD200 (Costello et al., 2011) showed impaired LTP induction in hippocampal slices. Also, hippocampal slices isolated from mice deficient in DAP12, a microglial receptor-associated protein involved in phagocytosis, showed enhanced LTP (Roumier et al., 2004). Our data confirm a physiological role for microglia in the homeostatic regulation of neuronal excitability and synaptic plasticity in the healthy brain *in vivo* and further show that IKKβ is a mediator of this effect, most probably through the induction of NF-κB transcriptional activity.

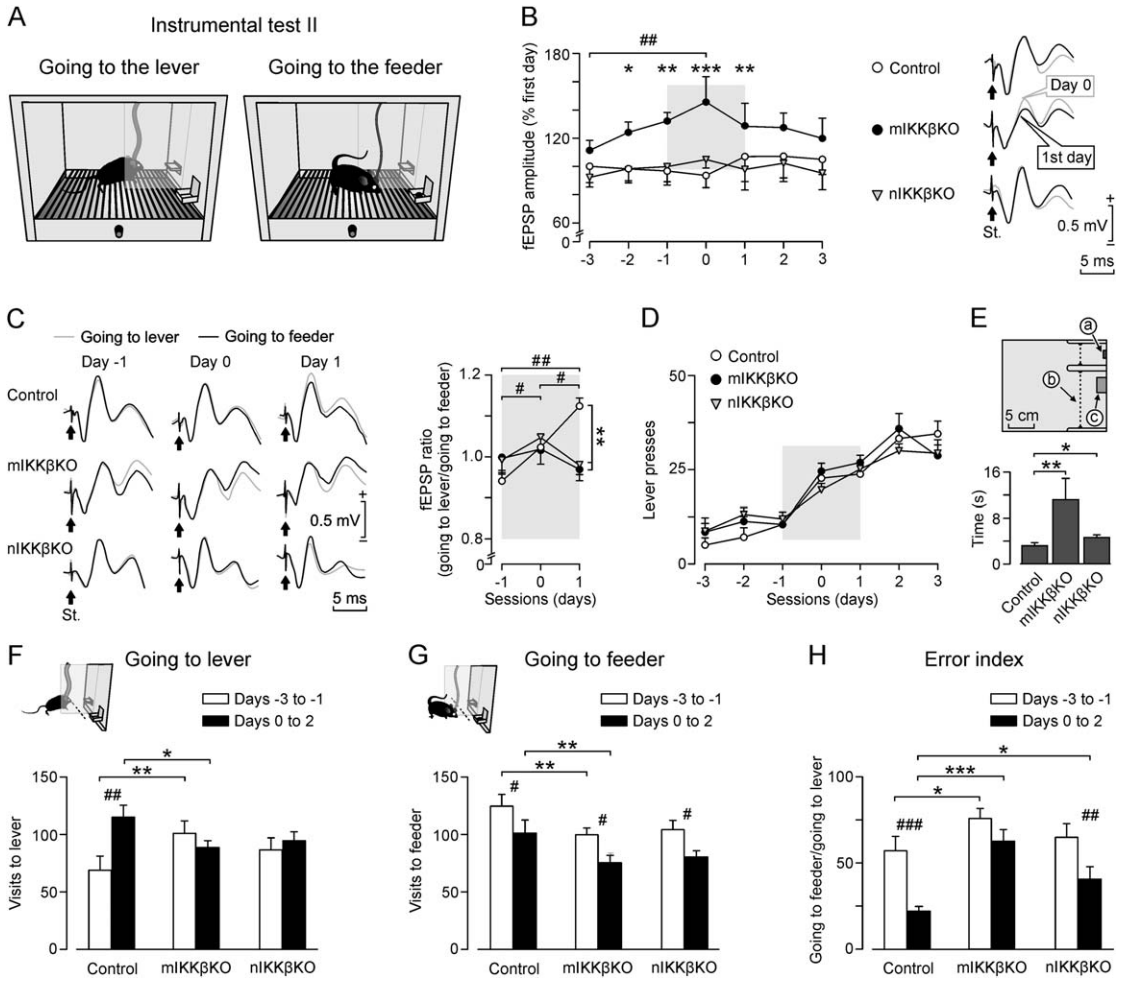

FIGURE 7: mIKKβKO and nIKKβKO mice show a selective impairment in the modification of appetitive behavior during instrumental reward learning that correlates with deficiency in hippocampal synaptic strength increase at the peak of acquisition. (A) Diagram of the Skinner box used in Instrumental test II to train mice with permanently-implanted electrodes. The box was the same as that shown in Fig. 6A, except for a partial Perspex wall that separates the lever from the feeder and a ceiling opening to allow free movement of the wires. Animals received CA3-CA1 synapse stimulation when approaching the lever or feeder. A photoelectric cell, crossing the chamber 5 cm from the feeder/lever, registered movements towards lever or feeder and automatically signaled intra-hippocampal stimulation. (B) Evolution of the fEPSP amplitudes measured in CA3-CA1 synapse immediately before the daily sessions (pre-session recordings) in the indicated days for both the mIKKβKO (black circles) and nIKKβKO mice (gray triangles), compared to controls (white circles) (n = 6 mice per group). Day 0 is defined as the first of the two days with 20 lever presses/session (criterion). Differences within the mIKKβKO group during the acquisition process (d-3 vs. d0: $^{\#\#}$, $P < 0.001$) and between the mIKKβKO and the control groups ($F_{(1,5,30)} = 2.738$, *, $P = 0.03$) are indicated. Representative pre-session fEPSPs recorded in CA1 of representative control, mIKKβKO and nIKKβKO mice on days 0 (dotted line) and 1 (line) of the acquisition process are illustrated. (C) Representation (left graph) and comparison (right graph) of the fEPSP ratio ("going-to-lever"/"going-to-feeder") in mIKKβKO and nIKKβKO mice, compared to controls (n = 6 mice per group) collected before (Day −1), during (Day 0) and after (Day 1) the peak of the acquisition process. Differences within the control group (d-1 vs. d0; d0 vs. d1: $^{\#}$, $P < 0.05$; d-1 vs. d1: $^{\#\#\#}$, $P < 0.001$) as well as between knockouts and control groups on day 1 are indicated (mIKKβKO vs. control: $F_{(1,5,10)} = 8.902$, **, $P = 0.006$; nIKKβKO vs. control: $F_{(1,5,10)} = 12.094$, **, $P = 0.002$). (D) Total lever presses by control (white circles), mIKKβKO (black circles) and nIKKβKO (gray triangles) (n = 6 per group) mice at the indicated days. (E) Graph illustrating the time (s) spent by control, mIKKβKO and nIKKβKO mice between the lever release and visit to the feeder on day 2. Differences between the control and the knockout groups (, $P = 0.008$; *, $P = 0.032$) are illustrated. A schematic representation of the Instrumental test II is shown above the graph. The values measured in the graph represent the time spent by each group to cross the photoelectric cell (b, dotted line) when leaving the lever (release the lever) (a) to feeder (c). (F) Graph illustrating the total number of visits to the lever, 3 days before (white) and 3 days after (black) criterion was reached (day 0) for the control, mIKKβKO and nIKKβKO mice (n = 6 per group). Differences within the control group ($^{\#\#}$, $P = 0.002$) and between the mIKKβKO and control groups are indicated ($F_{(1,17,17)} = 9.229$, **, $P = 0.007$). (G) Graph illustrating the total number of visits to the feeder 3 days before (white) and 3 days after (black) criterion was reached (day 0) for the control, mIKKβKO and nIKKβKO mice (n = 6 per group). Differences within the control (#, $P = 0.015$), mIKKβKO ($^{\#}$, $P = 0.013$) and nIKKβKO ($^{\#}$, $P = 0.013$) groups and between the mIKKβKO and control group ($F_{(1,17,17)} = 11.066$, **, $P = 0.004$) are indicated. (H) Graph illustrating the error index, defined as the ratio of going-to-feeder/going-to-lever, 3 days before (white) and 3 days after (black) criterion was reached (day 0). Differences within the control ($^{\#\#\#}$, $P < 0.001$) and nIKKβKO ($^{\#\#}$, $P < 0.01$) groups and between the two knockouts and the control group (mIKKβKO vs. control: $F_{(1,7,17)} = 4.564$, *, $P = 0.047$; nIKKβKO vs. control: $F_{(1,17,17)} = 0.919$, $P = 0.351$) are indicated. Data are shown as mean ± SEM and statistical analysis was made by two way ANOVA, repeated measures (B, D, F, G, H) or Mann Whitney Rank Sum test (E) for comparisons between the groups (*) and Holm Sidak method for comparisons within the groups between the different sessions ($^{\#}$).**

The role of NF-κB in the brain has been intensively studied centering on its functions in neurons. Studies of hippocampal slices from transgenic mice showed that neuronal NF-κB activity is not necessary for the induction of LTP but is required for the maintenance of late LTP (Kaltschmidt et al., 2006; O'Mahony et al., 2006), a process that models the initial phase of memory formation and is dependent upon gene expression (Citri and Malenka, 2008). Consistent with this, hippocampal slices from nIKKβKO mice also showed normal induction but impaired late LTP, as measured 2–3 h afterward (our unpublished results). Here we extended these results into an *in vivo* setting in freely moving mice by measuring the induction of LTP in two consecutive daily HFS sessions. nIKKβKO mice showed normal synaptic function, as measured by input/output curves, paired pulse facilitation and the initial induction of LTP by the first HFS session (Fig. 4). However, nIKKβKO mice were resistant to subsequent LTP induction (Fig. 4). Taken together, the available *ex vivo* and *in vivo* data show that neuronal NF-κB-mediated gene transcription is necessary for the maintenance of late LTP.

In contrast to neuronal NF-κB, the role of microglial NF-κB in the brain under physiological conditions has not been investigated. Surprisingly, mIKKβKO mice showed enhanced short-term plasticity (PPF) and increased LTP following both HFS sessions, with neuronal excitability recovering to control levels between sessions. These findings support the conclusion that IKKβ expressed by microglia is sufficient to regulate neuronal activity in short and long-term plasticity mechanisms.

Insight into the effector mechanism by which microglial IKKβ controls neuronal excitability comes from studies of cytokine function in the brain (Hiscott et al., 1993). IL-1β is an NF-κB-inducible gene that is expressed in the hippocampus during LTP (Schneider et al., 1998) and hippocampal-dependent learning and memory processes where it is specifically produced by $CD11b^{+}$-enriched microglia (Williamson et al., 2011). Correctly regulated IL-1β expression is needed to ensure proper hippocampal function; either reduced or increased levels result in impairments in neural plasticity and memory performance (Katsuki et al., 1990; Avital et al., 2003). Furthermore, defects in LTP and hippocampal-dependent cognitive function observed in CX3CR1-deficient mice are rescued by IL-1β inhibition (Rogers et al., 2011). Our finding that brains from mIKKβKO mice showed reduced RNA transcripts for IL-1β, not other NF-κB targets, suggests that microglial NF-κB activity regulates hippocampal neuronal excitability and synaptic plasticity through the induction of IL-1β expression.

The role of NF-κB in hippocampus-dependent learning and memory tasks has been extensively studied in mice constitutively deficient in the p50 subunit of NF-κB in all cell types but with conflicting results (reviewed by Snow et al., 2013). Only few studies have addressed the contribution of NF-κB in different CNS cell types to cognitive function. Neuron-specific inhibition of NF-κB was found to impair spatial memory formation (Kaltschmidt et al., 2006; O'Mahony et al., 2006) while astroglia-specific inhibition of NF-κB showed delayed spatial learning and impaired cued fear memory (Bracchi-Ricard et al., 2008). However, the role of microglial NF-κB activity has not been previously studied. Our results in conditional IKKβ knockout mice clearly illustrate the differential contribution of NF-κB by different cell lineages to behavior. In the passive avoidance task, a test for contextual fear memory that involves mainly the dorsal hippocampus and amygdaloid complex (Phillips and LeDoux, 1992; Baarendse et al., 2008), both mIKKβKO and nIKKβKO mice showed increased fear memory compared with controls, but with different kinetics. mIKKβKO mice showed increased short-term fear responses but normal extinction of the memory indicating a role for microglial NF-κB in the initial consolidation of fear memory. In contrast, nIKKβKO mice showed equivalent short-term but markedly increased long-term fear responses indicating a role for neuronal NF-κB in the extinction of fear memory to the sensory footshock experience, a process known to be hippocampus-dependent (Baarendse et al., 2008). Interestingly, LTP and contextual fear conditioning have been found to share common molecular mechanisms (Schafe et al., 1999), so our combined observations are consistent with a role for microglial NF-κB in the initial phases of memory formation and a requirement for neuronal NF-κB in the long-term maintenance of synaptic plasticity and modification of fear memory, which are known to depend on *de novo* protein synthesis.

The participation of microglial and neuronal IKKβ in specialized hippocampal function was further revealed by instrumental conditioning, which tested the animals ability to identify the causal association between an action (appetitive behavior, going-to-lever) and an outcome (consummatory behavior, going-to-feeder, eating) and to integrate sensory information into this relationship, processes known to depend on the integrity of the dorsal hippocampus (Corbit and Balleine, 2000; Moyer et al., 1990). First, while both mutants learned the simple association between action and outcome, albeit with a delay in the mIKKβKO, a process that is hippocampus independent (Corbit and Balleine, 2000), neither strain optimally incorporated sensory information to improve performance in the light/dark paradigm in the same way as controls (Fig. 6I, J). Second, we show that neither mutant strain showed modification of appetitive behavior, a hippocampus-dependent function (Flaherty et al., 1998), while hippocampus-independent consummatory behavior was

modified in the same way as in controls. The deficit in appetitive behavior correlated in both strains with an absence of increases in synaptic strength at the CA3-CA1 synapse at the peak of the acquisition process, specifically 1 day after criterion day (day 0) (Fig. 7C). Interestingly, fEPSP changes and deficits in appetitive behavior were similar in the two strains and did not display the temporal differences detected during LTP (Figs. 3E and 4C), a finding that supports previous evidence that LTP and behavioral performance are not always correlated (Huang et al., 1995; Migaud et al., 1998; Sahún et al., 2007; Vega-Flores et al., 2014). Therefore, our results identify a mechanistic dissociation between appetitive and consummatory behavior in mice, as well as a specific complementary role for microglial and neuronal IKKβ in hippocampal-dependent modification of appetitive behavior during associative learning. Taken together the results from passive avoidance and instrumental conditioning paradigms show that microglial and neuronal IKKβ are independently required for proper modification of behavior that relies on hippocampus function.

This study defines a novel functional role for microglia in the regulation of hippocampal synaptic plasticity and associative learning in the healthy intact brain. The finding that microglial IKKβ depletion affected neuronal excitability as well as short-term and long-term synaptic plasticity in the mouse hippocampus is fully consistent with a newly emerging role for microglia in homeostatic regulation of synaptic function (reviewed by Schafer et al., 2013). Further studies are needed to define whether canonical NF-κB signaling in microglia participates in the direct control of neurotransmission in the healthy brain and whether defects can lead to the development of brain pathology.

Acknowledgment

Grant sponsor: Spanish MINECO; Grant numbers: BFU2011-29089 and BFU2011-29286; Grant sponsor: Junta de Andalucía; Grant numbers: BIO122; CVI 2487; and P07-CVI-02686; Grant sponsor: EU FP7 REGPOT NeuroSign project; Grant number: 264083; Grant sponsor: Hellenic Republic Ministry of Education - General Secretariat of Research & Technology (GSRT), National Action Cooperation Project; Grant number: 09SYN-21-609. V. Kyrargyri was a predoctoral visitor to Pablo de Olavide University supported by a fellowship from the Theodorou Theohari Kotsika Foundation, Greece. G. Vega-Flores was a predoctoral student supported with a Spanish MINECO BFU2008-00889 fellowship. The authors wish to thank David Attwell and Harald Neumann for discussions and critical reading of the manuscript. They also thank the following persons for their valuable help; José Antonio Santos with the experimental set-up, María Sánchez-Enciso with animal handling and care, Maria Karamita with immunohistochemistry, Maria Evangelidou with FACS analysis, and Marina Papoulia with characterization of IKKβ levels in brain areas from nIKKβKO mice.

References

Avital A, Goshen I, Kamsler A, Segal M, Iverfeldt K, Richter-Levin G, Yirmiya R. 2003. Impaired interleukin-1 signaling is associated with deficits in hippocampal memory processes and neural plasticity. Hippocampus 13:826–834.

Baarendse PJ, van Grootheest G, Jansen RF, Pieneman AW, Ögren SO, Verhage M, Stiedl O. 2008. Differential involvement of the dorsal hippocampus in passive avoidance in C57bl/6J and DBA/2J mice. Hippocampus 18:11–19.

Boillée S, Yamanaka K, Lobsiger CS, Copeland NG, Jenkins NA, Kassiotis G, Kollias G, Cleveland DW. 2006. Onset and progression in inherited ALS determined by motor neurons and microglia. Science 312:1389–1392.

Bracchi-Ricard V, Brambilla R, Levenson J, Hu WH, Bramwell A, Sweatt JD, Green EJ, Bethea JR. 2008. Astroglial nuclear factor-kappaB regulates learning and memory and synaptic plasticity in female mice. J Neurochem 104: 611–623.

Cho IH, Hong J, Suh EC, Kim JH, Lee H, Lee JE, Lee S, Kim CH, Kim DW, Jo EK. 2008. Role of microglial IKKbeta in kainic acid-induced hippocampal neuronal cell death. Brain 131(Pt 11):3019–3033.

Citri A, Malenka RC. 2008. Synaptic plasticity: Multiple forms, functions, and mechanisms. Neuropsychopharmacology 33:18–41.

Corbit LH, Balleine BW. 2000. The role of the hippocampus in instrumental conditioning. J Neurosci 20:4233–4239.

Costello DA, Lyons A, Denieffe S, Browne TC, Cox FF, Lynch MA. 2011. Long term potentiation is impaired in membrane glycoprotein CD200-deficient mice: A role for Toll-like receptor activation. J Biol Chem 286: 34722–34732.

Davalos D, Grutzendler J, Yang G, Kim JV, Zuo Y, Jung S, Littman DR, Dustin ML, Gan WB. 2005. ATP mediates rapid microglial response to local brain injury in vivo. Nat Neurosci 8:752–758.

Emmanouil M, Taoufik E, Tseveleki V, Vamvakas SS, Tselios T, Karin M, Lassmann H, Probert L. 2009. Neuronal I kappa B kinase beta protects mice from autoimmune encephalomyelitis by mediating neuroprotective and immunosuppressive effects in the central nervous system. J Immunol 183: 7877–7889.

Flaherty CF, Coppotelli C, Hsu D, Otto T. 1998. Excitotoxic lesions of the hippocampus disrupt runway but not consummatory contrast. Behav Brain Res 93:1–9.

Fridmacher V, Kaltschmidt B, Goudeau B, Ndiaye D, Rossi FM, Pfeiffer J, Kaltschmidt C, Israel A, Memet S. 2003. Forebrain-specific neuronal inhibition of nuclear factor-kappaB activity leads to loss of neuroprotection. J Neurosci 23:9403–9408.

Gruart A, Benito E, Delgado-García JM, Barco A. 2012. Enhanced cAMP response element-binding protein activity increases neuronal excitability, hippocampal long-term potentiation, and classical eyeblink conditioning in alert behaving mice. J Neurosci 32:17431–17441.

Hasan MT, Hernández-González S, Dogbevia G, Treviño M, Bertocchi I, Gruart A, Delgado-García JM. 2013. Role of motor cortex NMDA receptors in learning-dependent synaptic plasticity of behaving mice. Nat Commun 4: 2258.

Hiscott J, Marois J, Garoufalis J, D'Addario M, Roulston A, Kwan I, Pepin N, Lacoste J, Nguyen H, Bensi G. 1993. Characterization of a functional NF-kappa B site in the human interleukin 1 beta promoter: Evidence for a positive autoregulatory loop. Mol Cell Biol 13:6231–6240.

Hoffmann A, Baltimore D. 2006. Circuitry of nuclear factor kappaB signaling. Immunol Rev 210:171–186.

Huang YY, Kandel ER, Varshavsky L, Brandon EP, Qi M, Idzerda RL, McKnight GS, Bourtchouladze R. 1995. A genetic test of the effects of mutations in

PKA on mossy fiber LTP and its relation to spatial and contextual learning. Cell 83:1211–1222.

Imai Y, Kohsaka S. 2002. Intracellular signaling in M-CSF-induced microglia activation: Role of Iba1. Glia 40:164–174.

Ji K, Akgul G, Wollmuth LP, Tsirka SE. 2013. Microglia actively regulate the number of functional synapses. PLoS One 8:e56293.

Jurado-Parras MT, Sánchez-Campusano R, Castellanos NP, del-Pozo F, Gruart A, Delgado-García JM. 2013. Differential contribution of hippocampal circuits to appetitive and consummatory behaviors during operant conditioning of behaving mice. J Neurosci 33:2293–2304.

Kaltschmidt B, Kaltschmidt C. 2009. NF-kappaB in the nervous system. Cold Spring Harb Perspect Biol 1:a001271.

Kaltschmidt B, Ndiaye D, Korte M, Pothion S, Arbibe L, Prüllage M, Pfeiffer J, Lindecke A, Staiger V, Israël A, Kaltschmidt C, Mémet S. 2006. NF-kappaB regulates spatial memory formation and synaptic plasticity through protein kinase A/CREB signaling. Mol Cell Biol 26:2936–2946.

Katsuki H, Nakai S, Hirai Y, Akaji K, Kiso Y, Satoh M. 1990. Interleukin-1 beta inhibits long-term potentiation in the CA3 region of mouse hippocampal slices. Eur J Pharmacol 181:323–326.

Kettenmann H, Hanisch UK, Noda M, Verkhratsky A. 2011. Physiology of microglia. Physiol Rev 91:461–553.

Lee SJ, Zhou T, Choi C, Wang Z, Benveniste EN. 2000. Differential regulation and function of Fas expression on glial cells. J Immunol 164:1277–1285.

Li Y, Du XF, Liu CS, Wen ZL, Du JL. 2012. Reciprocal regulation between resting microglial dynamics and neuronal activity in vivo. Dev Cell 23:1189–1202.

Li ZW, Omori SA, Labuda T, Karin M, Rickert RC. 2003. IKK beta is required for peripheral B cell survival and proliferation. J Immunol 170:4630–4637.

Madroñal N, López-Aracil C, Rangel A, del Río JA, Delgado-García JM, Gruart A. 2010. Effects of enriched physical and social environments on motor performance, associative learning, and hippocampal neurogenesis in mice. PLoS One 5:e11130.

Mattson MP, Camandola S. 2001. NF-kappaB in neuronal plasticity and neurodegenerative disorders. J Clin Invest 107:247–254.

Meffert MK, Chang JM, Wiltgen BJ, Fanselow MS, Baltimore D. 2003. NF-kappa B functions in synaptic signaling and behavior. Nat Neurosci 6:1072–1078.

Migaud M, Charlesworth P, Dempster M, Webster LC, Watabe AM, Makhinson M, He Y, Ramsay MF, Morris RG, Morrison JH. 1998. Enhanced long-term potentiation and impaired learning in mice with mutant postsynaptic density-95 protein. Nature 396:433–439.

Minichiello L, Korte M, Wolfer D, Kuhn R, Unsicker K, Cestari V, Rossi-Arnaud C, Lipp HP, Bonhoeffer T, Klein R. 1999. Essential role for TrkB receptors in hippocampus-mediated learning. Neuron 24:401–414.

Moyer JR Jr, Deyo RA, Disterhoft JF. 1990. Hippocampectomy disrupts trace eye-blink conditioning in rabbits. Behav Neurosci 104:243–252.

Nakajima K, Tohyama Y, Kohsaka S, Kurihara T. 2001. Ability of rat microglia to uptake extracellular glutamate. Neurosci Lett 307:171–174.

Neumann H, Kotter MR, Franklin RJ. 2009. Debris clearance by microglia: An essential link between degeneration and regeneration. Brain 132(Pt 2):288–295.

Nimmerjahn A, Kirchhoff F, Helmchen F. 2005. Resting microglial cells are highly dynamic surveillants of brain parenchyma in vivo. Science 308:1314–1318.

O'Mahony A, Raber J, Montano M, Foehr E, Han V, Lu SM, Kwon H, LeFevour A, Chakraborty-Sett S, Greene WC. 2006. NF-kappaB/Rel regulates inhibitory and excitatory neuronal function and synaptic plasticity. Mol Cell Biol 26:7283–7298.

Paolicelli RC, Bolasco G, Pagani F, Maggi L, Scianni M, Panzanelli P, Giustetto M, Ferreira TA, Guiducci E, Dumas L. 2011. Synaptic pruning by microglia is necessary for normal brain development. Science 333:1456–1458.

Park JM, Greten FR, Li ZW, Karin M. 2002. Macrophage apoptosis by anthrax lethal factor through p38 MAP kinase inhibition. Science 297:2048–2051.

Phillips RG, LeDoux JE. 1992. Differential contribution of amygdala and hippocampus to cued and contextual fear conditioning. Behav Neurosci 106:274–285.

Potter MC, Elmer GI, Bergeron R, Albuquerque EX, Guidetti P, Wu HQ, Schwarcz R. 2010. Reduction of endogenous kynurenic acid formation enhances extracellular glutamate, hippocampal plasticity, and cognitive behavior. Neuropsychopharmacology 35:1734–1742.

Ransohoff RM, Brown MA. 2012. Innate immunity in the central nervous system. J Clin Invest 122:1164–1171.

Rogers JT, Morganti JM, Bachstetter AD, Hudson CE, Peters MM, Grimmig BA, Weeber EJ, Bickford PC, Gemma C. 2011. CX3CR1 deficiency leads to impairment of hippocampal cognitive function and synaptic plasticity. J Neurosci 31:16241–16250.

Roumier A, Béchade C, Poncer JC, Smalla KH, Tomasello E, Vivier E, Gundelfinger ED, Triller A, Bessis A. 2004. Impaired synaptic function in the microglial KARAP/DAP12-deficient mouse. J Neurosci 24:11421–11428.

Sahún I, Delgado-García JM, Amador-Arjona A, Giralt A, Alberch J, Dierssen M, Gruart A. 2007. Dissociation between CA3-CA1 synaptic plasticity and associative learning in TgNTRK3 transgenic mice. J Neurosci 27: 2253–2260.

Schafe GE, Nadel NV, Sullivan GM, Harris A, LeDoux JE. 1999. Memory consolidation for contextual and auditory fear conditioning is dependent on protein synthesis, PKA, and MAP kinase. Learn Mem 6:97–110.

Schafer DP, Lehrman EK, Kautzman AG, Koyama R, Mardinly AR, Yamasaki R, Ransohoff RM, Greenberg ME, Barres BA, Stevens B. 2012. Microglia sculpt postnatal neural circuits in an activity and complement-dependent manner. Neuron 74:691–705.

Schafer DP, Lehrman EK, Stevens B. 2013. The "quad-partite" synapse: Microglia-synapse interactions in the developing and mature CNS. Glia 61:24–36.

Schneider H, Pitossi F, Balschun D, Wagner A, del Rey A, Besedovsky HO. 1998. A neuromodulatory role of interleukin-1beta in the hippocampus. Proc Natl Acad Sci USA 95:7778–7783.

Snow WM, Stoesz BM, Kelly DM, Albensi BC. 2013. Roles for NF-kappaB and gene targets of NF-kappaB in synaptic plasticity, memory, and navigation. Mol Neurobiol 49:757–770.

Stellwagen D, Malenka RC. 2006. Synaptic scaling mediated by glial TNF-alpha. Nature 440:1054–1059.

Tremblay ME, Lowery RL, Majewska AK. 2010. Microglial interactions with synapses are modulated by visual experience. PLoS Biol 8:e1000527.

Vallabhapurapu S, Karin M. 2009. Regulation and function of NF-kappaB transcription factors in the immune system. Annu Rev Immunol 27:693–733.

Valles-Ortega J, Duran J, Garcia-Rocha M, Bosch C, Saez I, Pujadas L, Serafin A, Cañas X, Soriano E, Delgado-García JM, Gruart A, Guinouart J. 2011. Neurodegeneration and functional impairments associated with glycogen synthase accumulation in a mouse model of Lafora disease. EMBO Mol Med 3:667–681.

Vega-Flores G, Rubio SE, Jurado-Parras MT, Gómez-Climent MÁ, Hampe CS, Manto M, Soriano E, Pascual M, Gruart A, Delgado-García JM. 2014. The GABAergic septohippocampal pathway is directly involved in internal processes related to operant reward learning. Cereb Cortex 24:2093–2107.

Wake H, Moorhouse AJ, Jinno S, Kohsaka S, Nabekura J. 2009. Resting microglia directly monitor the functional state of synapses in vivo and determine the fate of ischemic terminals. J Neurosci 29:3974–3980.

Whishaw IQ, McKenna JE, Maaswinkel H. 1997. Hippocampal lesions and path integration. Curr Opin Neurobiol 7:228–234.

Williamson LL, Sholar PW, Mistry RS, Smith SH, Bilbo SD. 2011. Microglia and memory: Modulation by early-life infection. J Neurosci 31:15511–15521.

Zucker RS, Regehr WG. 2002. Short-term synaptic plasticity. Annu Rev Physiol 64:355–405.